Observers Who Read Their Universe into Existence: Finite Consensus and the Reconstruction of Standard Physics

Bernhard Mueller[1,*] Mario Poneder Alexander Osika[2] Kai Xue
Ben Cassie Peter Nguyen Jinwook Kim[3] David Matscheko
Daniel Ari Friedman[4,5] Jonathan Hill William T. Glynn Maarten Antonie Visser
Kale Arnav Anirudha Brieuc de La Fournière

November 23, 2026 · Paper release: r2073

[1]Pragma Research Inc. [2]EtherWorks [3]Oraclizer Labs [4]Active Inference Institute [5]FractiAI
[*]Corresponding author: bernhard@floatingpragma.ai

Abstract

Observer Patch Holography formulates self-creation as a fixed-point condition. Observers discover the laws of their history and build a realization that reproduces it, including the builders. We implement a finite computation on a spherical network of twelve-port cells. From detector records alone the three spatial directions of a programmed scalar wave can be recovered. With a material clock, the prescribed refinement has a flat relativistic 3+1-dimensional field limit on bounded times and momentum bands.

Lean proofs give one public outcome for terminating, locally confluent repairs from a fixed record. On a finite complex measurement algebra, normalized probabilities additive on coexisting effects obey the Born rule for a unique density matrix. Averaging local measurement outcomes preserves the remote state. Quantum correlations attain the sharp CHSH bound $2\sqrt{2}$. The cell has three independent slow responses. Twelve independent port currents that close in a faithful, complete compact algebra and implement cell rotations internally have the Standard Model gauge Lie type.

Given the small-region area and matter-entropy relations, entropy stationarity at fixed proper volume in every local frame yields the Einstein equation up to a cosmological constant on a common Lorentzian spacetime with conserved stress. In a separate semiclassical model, two quantum fields source independently measured geometry under supplied Einstein evolution. Deriving universal curvature and realizing the closure condition on our observable history are tests of the full theory.

Keywords: foundations of physics; Observer Patch Holography; finite consensus; self-reference; executable model; quantum records; emergent spacetime; gauge structure; particle physics; Einstein dynamics.

1 Introduction

Imagine receiving the reports of eight stations with their coordinates erased. Each station can launch a pulse, count local clock events and report where the pulse was detected. Which stations are neighbours? How many directions can a pulse travel? On the finite computer studied here, the first round of detector counts answers both questions. The eight stations have twelve links and

three independent binary coordinates. With the walk rule and a separately calibrated material clock, these coordinates predict all twenty-four distributions measured at three later clock readings. The largest absolute error in a recorded probability is 0.001022. Merging the stations along any one recovered direction forces an error of at least 0.11377 in the corresponding population predictions [68].

The hardware underneath this experiment is a spherical network of icosahedral cells. Each cell has twelve ports, and each connecting seam carries a finite memory. The wiring specifies which ports can interact. The positions just reconstructed describe the propagation of a scalar excitation under a particular routing of those interactions. For a given preparation and schedule, the computation deterministically evolves the state between measurements and calculates the probabilities of the possible detector records. An observer inside the experiment learns a propagation law from those records. On bounded times and momentum bands, refining the routing gives the free Klein–Gordon equation in flat 3+1-dimensional spacetime. The routing is part of the apparatus [68].

There is a second question an observer could ask of its records. Can it recover the machinery that made them? In a finite carrier experiment, event logs and a specified set of probes determine the twelve ports, their thirty internal seams and the local repair rule. Running the recovered description reproduces the measured invariants through two iterations. The closure hypothesis extends this kind of test to an entire history. Its observers must recover a specification and build a realization whose records and responses agree with the history containing those observers, their discovery and their construction. This is the physical meaning of self-creation proposed here (Section 2) [2].

1.1 Mission

The mission of OPH is a consistent and complete, formal and rigorous theory of reality. Its proposed complete history has no external starting point: it closes on itself. A successful theory must meet four conditions.

1. **Consistent.** Exhibit a history and its internal realization that satisfy the closure condition, and verify the identification. An explicit model witnesses the consistency of its stated assumptions.

2. **Explicit.** The complete recovered specification fixes its consequences. Every design choice and calibration is declared; quantities claimed as independent predictions are not inserted through those inputs.

3. **Complete**, in the sense Einstein, Podolsky and Rosen gave the word [21]. Every element of physical reality has a counterpart in the theory, and every measured quantity is derived.

4. **Correct.** Derived values agree with measurement, and new predictions are frozen before they are tested.

The mission ranges from the existence of an inhabited history and the possibility of experience to the number of spatial directions, quantum statistics, forces, particles, gravity and cosmology. This range specifies what the proposed account must explain; it does not turn a finite model or a conditional theorem into a derivation of every item. In particular, a three-dimensional carrier response needs a physical position map, and an operational observer needs an additional account before any claim about phenomenal qualities follows. Table 12 gives these distinctions alongside the physical results.

OPH does not claim to be the only theory with these properties. The four conditions organize this paper. Consistency is tested through the closure hypothesis and the executable model

(Section 2) and through the machine-checked results of Section 13. Specification and parameter ancestry are tested through the closure coordinates of Section 10.3. Completeness is the ledger of realized results and physical obligations in Section 11. Correctness is decided by the frozen predictions and tests of Section 12.

1.2 Consistency through local repair

Local repair is the engine of the proposal. A finite observer has no global view. It holds a patch of local state, reads the boundary shared with neighbors, retains records and repairs disagreements while protecting what has been recorded. A fact becomes public when every authorized comparison preserves it. The finite consensus theorem gives such records a canonical normal form independent of the repair schedule. Observer Patch Holography (OPH) asks whether the world we measure can be reconstructed from this kind of compatible local access. Quantum probability, Lorentzian kinematics, gravitational dynamics and gauge structure enter standard physics through distinct mathematical inputs [22, 23, 24, 59, 66]; OPH tests whether one observer architecture can carry their public readouts. Space, time, matter and classical objects are effective descriptions of what observers can measure and jointly interpret. In this interpretation, spacetime geometries and quantum field theories describe relations among compatible records; the proposal assumes no prior observer-independent continuum.

The twelve-port carrier makes this idea concrete. Optimal readout of a three-dimensional response selects its incidence, and its normalized repair response has a three-dimensional slow quotient, a candidate carrier for spatial position. Under the further premise that a faithful complete reversible current implements the carrier's rechartings internally, its Lie algebra has type $\mathfrak{u}(1) \oplus \mathfrak{su}(2) \oplus \mathfrak{su}(3)$. Three directions and the Standard Model gauge type thus arise as different constraints on the same cell response. On the finite matter module, six protected flux classes correspond to centre characters of Standard Model representations. Identifying them with laboratory excitations requires charge and transport measurements on the same states.

At continuum scale, consistency links matter and geometry. If one history supplies conserved stress and makes every local null direction obey the same curvature–stress balance, tensor completion yields the Einstein equation up to a cosmological constant. Obtaining that balance, the entropy response and a common physical geometry from the finite source is a separate requirement. OPH's unifying hypothesis is that the full dynamics of nature are the conditions under which one self-reading process keeps its records coherent through local repair.

On the same spherical hardware an observer can ask whether two loads form a pair. One instrument writes just the answer to that question. Another writes which seam holds the pair. Both give identical probabilities for finding a pair. Their effect on the pair can be measured by reading the emitting seam after further evolution. The joint probabilities are 0.0182640 and 0.1029264 for an initial yes and a final pair on that seam. The observer can distinguish these instruments from successive records alone. This is a circuit realization of projective conditioning (Theorem 4.5 and Figure 6).

A prepared pair also acts as a probe of the cell currents. Applying opposite pulses of a rotation-selected current changes the probabilities of the terminal seam records. The twelve generators close under commutators on the two accessible triplets (Section 8.2). On ordinary blank seams a different preparation carries a coherent two-state orbital through two cell boundaries. A guided reunion compares two material clocks by reading their counts on one shared seam (Section 6.5). Here an excitation, a current and an elapsed time each have a local preparation or readout by which another observer can check the claim.

Gravity poses a further experimental question. Does changing what the matter carries change

the geometry measured with an independent instrument? On a homogeneous spacetime with Einstein evolution supplied, two entangled preparations with identical individual field states give different radar and fixed-volume area readings. On the repair network a flying probe detects a correlation between seam memories, and local exchange can account for its response. A gravitational interpretation requires a curvature measurement sourced by the same calibrated stress (Section 9). Table 8 gives the preparations and hypotheses for these observer experiments.

1.3 Scope and order of the argument

The program has four logically different levels. Closure proposes that an inhabited history contains a recoverable account of its own operations. A source specification states the carrier, observer access, repair, record and state laws. Finite theorems and executable certificates determine what that specification does. Physical realization asks whether one such source has the observed fields, particles, clocks and responsive geometry. The implications run in that order; Table 1 states the result at each level.

Table 1: The OPH program and the status of its main implications.

Level	**Result on its stated domain**	**Physical requirement**
Closure	Finite consensus has an exact fixed-point packet theorem; a universe-level self-recovering history is proposed	A specified history and realization map satisfying the closure condition
Records and carrier	Canonical public records, conditional quantum identities, finite entropy laws of repair and an exact rank-three slow response	A common physical position, clock, energy and preparation map
Executable model	Interval Echo: the contrast-memory seam with its exact memory realization and a binding theorem on every federation, bound objects that persist in the agreed records, observer clocks whose reunions follow the proper-time forecast, agreement of overlapping observers and twelve closed port currents; the scalar channel with a prepared cage clock	An authenticated causal order with count and volume limits, one limiting speed for bound objects, a complete current menu and one common measurement of current and stress on a bound excitation
Gauge and matter	Complete-response premises force the Standard Model Lie type; protected defects carry exactly the particle centre classes; port phases give the global group	An interacting chiral field with the observed species, quark flavours and mixing
Gravity and cosmology	Null tomography and entropy premises imply the Einstein equation; finite capacity and pixel equations give conditional relations	The same source must supply conserved stress, responsive geometry, vacuum, scales and prospective observational matches

The finite results make OPH a concrete reconstruction program. Their composition into the observed universe is a separate mathematical and empirical claim. The specialist papers give the longer proofs, source executions and failed attachments [12, 11, 9, 67].

Finite theorems, complete source executions and physical interpretations answer different ques-

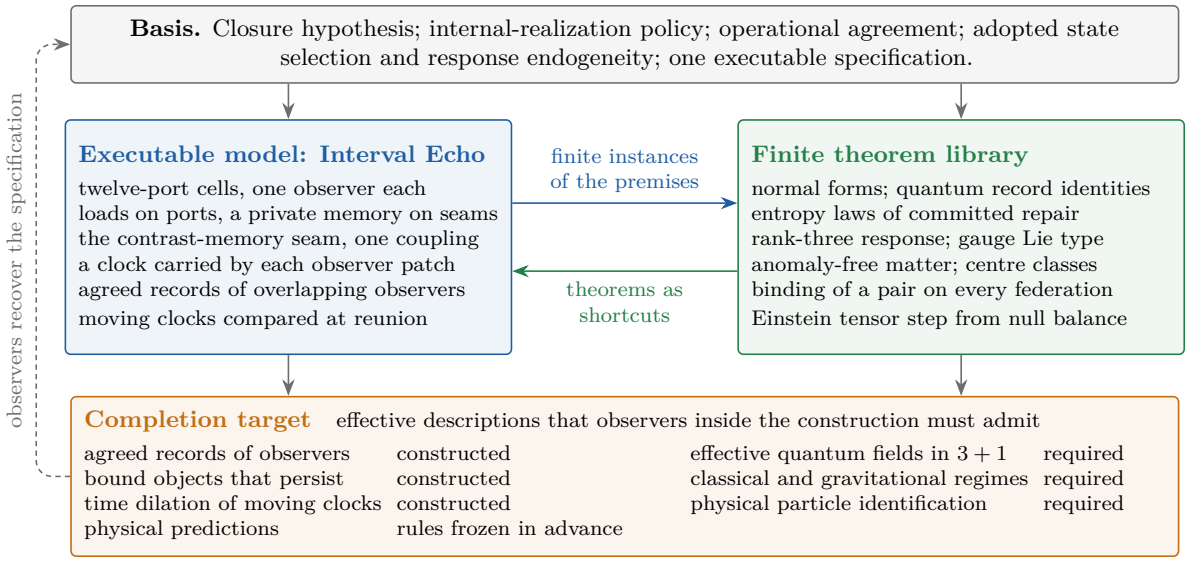


Figure 1: The proposed chain from protected records to physical laws. The finite theorems and the runs of the executable model constrain one specification; physical conclusions require compatible realization maps. The dashed arrow is the closure proposal: observers recover the specification from their records.

tions. We state each result's domain and supplied inputs where it is used; the detailed claim classes and verification methods are collected in Section 13.

A result of the executable model is stated on records: the observer, the record it holds and the probability the law gives for it. The state vector, its levels, the evolution parameter and positions in a sequence of events are tools of the calculation, and the text marks them as audit where they appear. No common clock is assumed; each observer counts its own events. The supplied parts of the construction are listed once, in Section 6.10.

Definition 1.1 (Physical realization map)**.** A physical realization map assigns finite public records, event data, currents, modular generators, and scales to physical records, spacetime events, laboratory currents, clocks, and units, preserving the algebraic operations, overlap restrictions, causal order, normalizations, and refinement relations consumed by the conclusion in question. A resemblance of spectra, dimensions, or symmetry names is insufficient.

The paper gives one mathematical representative of each step: the native repair rule and its contrast-memory law, the consensus normalizer, the spatial and gauge reductions, the finite matter representation and the Einstein tensor implication. Its status tables and prospective tests specify the physical conclusions. The companion construction and component papers carry implementation contracts and longer proofs [67, 1, 4, 5, 6, 8, 11, 9, 7, 13, 20, 2].

2 Closure and the source-specification hypothesis

This section states the interpretation and acceptance criterion: closure, the internal-realization policy, the additional state-selection and response-endogeneity principles, and the agreement condition, then explains why closure is tested through an executable model.

2.1 The closure hypothesis

The universe is modeled as a timeless, closed, self-referential structure in which the description and the described system are one object. Let $\mathfrak{U}$ be a complete inhabited history, let $D(\mathfrak{U})$ be an account of its architecture recoverable through completed records within it, and let R be an admissible realization of that account constructed inside $\mathfrak{U}$. The closure condition is

$$R(D(\mathfrak{U})) \;\cong\; \mathfrak{U}, \tag{1}$$

where $\cong$ is agreement in the observable and interventional structure: the records used to recover the description, and the responses of the realization to every admitted intervention, fit the world from which the account was recovered. Written as a fixed point of a universe-level closure operator, the condition reads $T(\mathfrak{U}) = \mathfrak{U}$. Observers infer the specification of their world, build hardware within it, and run that hardware; its execution realizes the same history, including its builders and their hardware. The identification of the construction-side and inhabited-side readings is the hypothesis. In this sense the structure reads itself into existence.

Within this hypothesis, no external computer runs the history and no additional time exists in which the whole is played. Host runtime used to check a model is part of our method of investigation, not an extra time coordinate of the universe described by that model. Repair order is a partial order on commits, an observer history is a chain of completed records, and that order is invariant under strictly increasing regradings, so affine time and proper time require their own calibration. Fixedness of the complete history permits changing states within it: the equation concerns the whole history and identifies no last instantaneous state with the universe.

A physical law is forced by a set of constraints if every admissible realization obeys it. For example, on the finite consensus branch the closure map is an affine idempotent. Its fixed points are exactly the packets supported on consensus normal forms [6]. This identifies a class of public records. To prove that closure singles out our observable Universe, every admitted fixed history would have to give the joint laws measured in our experiments, including those withheld from the reconstruction. Two microscopically different realizations could agree on all of those laws.

The finite reconstruction shows what can get lost in passing from records to a specification. Event logs distinguish the local icosahedral carrier from tetrahedral and octahedral controls. The retained routing records nevertheless admit two port gluings with different triangle counts and identical recorded bytes (Section 4). A measurement sensitive to those gluings would impose a further constraint. There is also a numerical closure condition $N = \log M_0(\mathfrak{U}_N)$, where N is the capacity budget of the regulated observer system and M_0 is the correctable-code capacity of its terminal public record. Base agreement, positivity and the carrier bound leave that capacity underdetermined [8]. A universe-level existence claim requires a specified history domain, an internal realization and a witness of Eq. (1) on that domain.

2.2 No outside

A self-contained realization must account internally for its operations and information access. This motivates a justification policy and two further constitutive principles; it does not logically derive those principles.

Justification policy. A premise is justified operationally when observers recover it and the specification implementing it runs and reproduces their measurements. The carrier, observer algebra, repair law and closure coordinates must meet that test. Their specification can be reconstructed from records or proposed as a design. In particular, using a twelve-port carrier does not require

a theorem that every possible realization must have twelve ports. A construction choice needs no uniqueness theorem unless uniqueness is claimed. Closure neither exempts a candidate from empirical tests nor proves its antecedents jointly realizable.

State-selection principle. On the declared feasible family, reference, observer cover and positive weights, adopt the information projection minimizing $\sum_p w_p D(\rho_p \| \tau_p)$. This is premise A3, motivated by least-informative inference but separately adopted when used as a physical selection law. The closure equation supplies no entropy functional or reference; even its identity-map specialization fixes both uniform and nonuniform states. Under A3, every minimizing local density has the union of feasible supports, and a feasible failure witness $b > 0$ gives an explicit selected-probability floor [9].

Response-endogeneity principle. The complete-response branch additionally requires each proper carrier recharting to be implemented by the connected response group, up to a unitary centralizer acting trivially on the response algebra. This is the endogeneity clause of A2, not a consequence of internal implementation alone. For example, twelve diagonal phase generators on $\mathbb{C}^{12}$ admit internal port permutations in $\mathrm{U}(1)^{12} \rtimes A_5$. These permutations act nontrivially on the abelian current algebra, whereas its inner automorphisms are trivial. This closed operation system fails the stronger endogeneity premise; it shows why that premise must be supplied. Theorem 8.1 uses it to select $\mathfrak{u}(1) \oplus \mathfrak{su}(2) \oplus \mathfrak{su}(3)$ under the stated complete-response hypotheses.

2.3 Agreement and the meaning of "our"

The justification policy fixes the operational test. Agreement says what counts as shared. Observers assign the same operational meaning to accepted data on shared boundaries, naturally under every restriction, recharting and refinement, and a record is public when it survives every authorized comparison (Theorem 4.4). "Our universe" is the world that this public record describes. Agreement in this sense is a definition and an acceptance criterion: it requires interpretation maps fixed independently of validation outcomes and preserving the declared joint and conditional statistics, including quantum correlations. It does not require a noncontextual table of outcomes for incompatible unperformed measurements. Agreement here is compatibility under specified comparisons and interventions, not a vote among observers or assent to a convenient interpretation. Its content includes the joint probabilities and the response to changed preparations. Calling space, time and matter operational descriptions does not make these constraints optional: once established by compatible records, they are public physical facts. The equations describe those relations and do not by themselves assert an additional material substrate beyond the specified process. The theorem library calls the interpretation clause of this condition A2. The basis reference distinguishes the closure hypothesis, agreement, adopted selection/endogeneity principles and executable specification, with the library's premise statements and their dictionary [84].

2.4 An entry point without a starting point

The exposition of this paper enters the loop at the executable specification. That choice reflects where observers stand, holding records and inferring, and it makes the account concrete. Closure states the internal realization contract; the adopted principles and specification then carry their own mathematical and empirical tests. The order of exposition is a logical entry point, not an event before the universe or a privileged temporal beginning of the self-referential loop. A pair of mutually determining equations such as $x = (y + 2)/2$, $y = (x + 2)/2$ fixes $x = y = 2$ with no first

value from which the other is manufactured; a calculator may approach the pair by iteration and someone may find it on a particular day, and neither belongs to the reason the answer is two.

The closure equation relates parts of one timeless object; it posits no backward signal in an external time coordinate. Observers recover the specification and later construct it in their own record order, and both stages belong to the same fixed point. In the terminating consensus theorems, repair descent supplies a well-founded order on the admitted updates for proving termination and comparing schedules; it is neither an observer's experienced time nor a universe-level clock.

What is reconstructed and what is constructed are two roles within this proposal. The observer who infers a law and the hardware that realizes it both belong to the candidate history. Finding that specification in a laboratory or checking it by computation occurs in the investigator's record order; neither supplies a temporal origin outside the history. If several specified closures satisfy the same tests, the results warrant that observational class without a uniqueness claim.

2.5 From closure to a testable specification

The executable observer gives the condition its finite meaning. A realization differs from a description because it carries the described dependencies under intervention: for a described update τ_a, realized operation F_a and fixed readout p, the one-step condition $p(F_a(s)) = \tau_a(p(s))$ extends by induction to every finite admitted sequence. A playback can match every frame of one history and fail this test as soon as a retained state is changed. The controls of Section 6 apply this test to the executable model: a changed preparation and a changed law, run through the same emitter and reader, change the agreed records.

Closure alone does not imply that a particular carrier, record law or initial state yields Standard Model physics. The executable-model hypothesis is the stronger claim that one simple, fully specified law does, and it is the form in which closure can fail. Its carrier architecture, refinement and composition, record instruments, memory law, scheduler, preparations and available controls are stated before testing. A failed specified law rejects that law and its tested interpretation; it reaches the wider proposal only when the rejected choice is proved necessary and exclusive. Changing the law, memory, state or decoder defines a new candidate.

The main candidate law of the executable model is Interval Echo. It runs the contrast-memory law of Section 3.4, the law of the reference candidate A-contrast-memory-spherical-v1, and adds a clock that each observer patch carries. The shared seam interaction reproduces particle stability: bound objects persist in free evolution, read on the agreed records of the observers, and the same law with the agreement energy removed loses them (Section 6.3). The clock of Interval Echo shows the time dilation of moving clocks on records that the observers make themselves (Section 6.5). Under a further candidate law on the same carrier an object on four seams is kept for every interval and carries a prepared clock, read from counts in units of the observer's own reference [68]. The construction supplies no selection of its couplings, and its calibrations are declared. The physical obligations of Section 11 are the tests the candidates have to pass on one process.

2.6 Specification and theorem premises

The architecture, record instruments, memory law, scheduler, preparation services and allowed interventions form a declared specification. Observers may infer or design these ingredients; mathematics determines their consequences, and comparison determines whether the resulting process matches observed physics. Declaring a primitive fixes the model under study. Its consequences require proofs, and its physical adequacy requires tests; a specified input must remain distinguishable from a consequence derived from other inputs. The carrier, memory and control laws need not be

uniquely selected by closure to be legitimate inputs. Their implementation and resource use must, however, belong to the process being studied.

Three premise families recur. A1 specifies the carrier, federation and response structure. A2 adds agreement on shared records and inner implementation of the complete response algebra. A3 adopts a least-informative state-selection principle on the stated feasible family. Closure alone proves neither the entropy minimizer nor the inner implementation assumption. Later theorems state which of these inputs they use and which additional hypotheses their conclusions require.

Quantum executions below use finite-dimensional complex Hilbert spaces, positive normalized density operators and completely positive instruments whose complete effects sum to the identity. These are explicit quantum premises, not consequences of classical normal-form uniqueness. A faithful reference is a strictly positive density operator $\rho > 0$; its modular flow is $\sigma_s(A) = \rho^{is} A \rho^{-is}$. The dimensionless parameter s requires a separate implemented calibration before it is read as duration.

The physical interpretation also fixes a domain: one prepared history, a family of interventions, or every allowed input state. These are inequivalent requirements. Complete quantum instruments must retain the reference systems and all outcomes needed for the chosen domain; a record history need not assign simultaneous values to unperformed incompatible measurements. Likewise, a stationary probability law, an instantaneous repair fixed point and the closure of an entire history are distinct. Host runtime, repair counts, modular parameters and measured duration are related only by an implemented clock calibration. The operational observer below is defined by access and record interfaces, without an additional claim about consciousness.

3 Finite observer services

The observer-service theorems use an operational observer and a twelve-port carrier with its specified repair law. These define the service domain. The executable model runs the same seam event without committing it: Section 3.4 states the seam law of its candidates and Section 6 their operation.

3.1 Patches, records and repair

Definition 3.1 (Observer patch)**.** An observer patch is a finite object with local state, an observable boundary map, durable records, readback, and a set of authorized repair moves. A patch sees a fragment of the world: its own state and the boundary data of its authorized overlaps.

Definition 3.2 (Overlap and repair)**.** For patches x_i, x_j with an authorized overlap $e = (i, j)$, both induced boundary records must agree for the pair to hold public data. A repair move changes local state while preserving protected readout. A configuration is a normal form when no authorized repair applies.

An observer in this sense is defined by its access and record interfaces. It reads, writes and retains records, and it uses retained records to choose its next operation. Nothing in the definition refers to a background space, a global clock or a pre-assigned list of particles. Those enter later as readouts that observers can share.

3.2 The twelve-port carrier

Each local carrier has twelve boundary ports, thirty seams and twenty oriented triangular faces. The incidence has a selection theorem that uses no topological template, Euler count, group action

or preassigned port count.

Theorem 3.3 (Icosahedral incidence from optimal readout)**.** *In a real three-dimensional response space, let unit vectors u_i read symmetric operators through $\mathrm{tr}(P_i X)$, $P_i = u_i u_i^{\mathsf{T}}$, with positive weights $\sum_i w_i = 1$, and put $M = \sum_i w_i |P_i\rangle\langle P_i|$. Informational completeness requires at least six distinct channels, and every choice obeys $\lambda_{\min}(M) \le 2/15$. With six channels, equality holds exactly for equal weights and the six icosahedral axes, up to an orthogonal frame. Exposing both signs gives twelve ports, positive overlap gives degree five and thirty edges, and the three-cliques give twenty faces. A deficit of at most 10^{-7} forces the same incidence, without forcing exact angles.*

Proof. Sym(3) has dimension six and each term of M has rank one. Each $P_i - I/3$ has squared norm $2/3$, so the trace-free compression of M has trace $2/3$ on five dimensions, which gives the bound. Equality forces $M(X) = (2X + \mathrm{tr}(X)I)/15$. At six channels the matrix F with columns $\sqrt{w_i}P_i$ is invertible and $F^{\mathsf{T}}M^{-1}F = I$: its diagonal gives $w_i = 1/6$ and its off-diagonal gives $(u_i \cdot u_j)^2 = 1/5$. The Gram matrix $I + S/\sqrt{5}$ then has a sign matrix with $S^2 = 5I$, whose unique switching class fixes the geometry [7]. □

The response dimension, the quadratic readout, both objectives, inverse ports and positive-overlap edges are premises, and a physical metric requires operational reconstruction. Carriers federate through typed seam algebras and coherent triple overlaps into a nerve with a degree-one bridge to an oriented sphere. Native current records recover the local Gram; executed cross-carrier routing uses supplied cell centres and tangent frames. A1 in the theorem library declares this carrier, federation and response layer.

Two exact features of the carrier enter later constructions. First, the proper rotation group of the icosahedral packet is the alternating group A_5, with sixty rotations acting on the twelve ports, and the real port-coefficient space decomposes without multiplicity as

$$P_{12} \;\cong_{A_5}\; \mathbf{1} \oplus \mathbf{3} \oplus \mathbf{3}' \oplus \mathbf{5}. \tag{2}$$

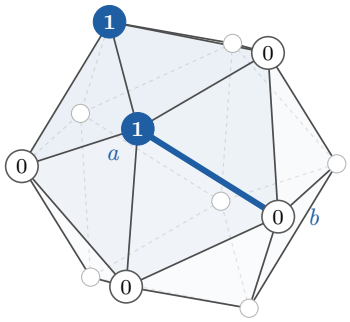
On the six-dimensional golden sector the spectral projectors have entries in $\frac{1}{20}\mathbb{Z}[\varphi]$, $\varphi = (1 + \sqrt{5})/2$, each is the entrywise Galois conjugate of the other, and both triplets are irreducible real representations of real type; the projectors, characters and irreducibility certificates are machine-checked [54, 1]. Second, record keeping is integer valued: a write appends $+1$, a retraction appends -1, and readback sums atomic events per port. A conservative repair transfers one unit across a seam whenever the oriented mismatch has magnitude at least two. With $V(x) = \sum_i x_i^2$, each such repair strictly decreases V by $2(d-1)$ for mismatch $d \ge 2$, so repair terminates. The native repair law of Section 3.3 also moves load to the floor and ceiling of the endpoint mean, but at difference one it waits or swaps by its coin, so the native process keeps moving while its quadratic cost stays fixed.

3.3 The native repair law

The seam event acts on integer loads. One carrier with twelve nonnegative integer loads of total two has 78 configurations, and the 66 binary configurations form an invariant shell. For an oriented seam (a, b) and a fair placement coin $c \in \{0, 1\}$ (Figure 2), the native repair law moves

$$d = x_a - x_b, \qquad j = \tfrac{1}{2}\big[d - (2c-1)(|d| \bmod 2)\big], \qquad y = x + j\,(e_b - e_a), \tag{3}$$

so load is conserved and the signed current j is the native observation. Conservation, one-step balance, a tie-break that reads no load and endpoint symmetry characterize this rule; on the total-two carrier they fix only the tie-break coin.



twelve ports, thirty seams, twenty faces; a binary load of total two (filled ports)

$d = x_a - x_b, \qquad j = \frac{1}{2}\big[d - (2c-1)(|d| \bmod 2)\big]$

d	$c=0$	$c=1$	effect of the attempt
2	1	1	balance
1	1	0	swap or wait
0	0	0	no move
-1	0	-1	wait or swap
-2	-1	-1	balance

The move j carries j units from a to b, and the fair coin c reads no load. At $|d| = 2$ the attempt lowers $V = \sum_i x_i^2$; at $|d| = 1$ it keeps V fixed, so the native process keeps moving. The seam drawn has $d = 1$.

Figure 2: The twelve-port carrier and its native repair. Left: the icosahedral incidence of the twelve ports, with thirty seams and twenty faces, in an orthographic view with back edges dashed; the filled ports carry a binary load of total two, and the drawn seam (a, b) has $d = 1$. Right: the seam rule for every mismatch the total-two carrier admits.

The event can be completed in two ways. Committed repair reads the event into a public record. Its quantum version is a record law, and seam locality, the classical law and the declared local number-phase and endpoint-swap covariance, a local phase symmetry of the repair channel, leave a convex family of them, each a table of five coherence multipliers [71]. The two laws used below have the same load update (3) and differ in which information they record. Write $p_e(x) = (x_a + x_b) \bmod 2$ for the parity of the seam's total load. Law C records the pair (c, j); law E records (c, j, p_e). Their Kraus operators are

$$L^C_{c,j} = \frac{1}{\sqrt{2}} \sum_{x:\, j(x,c)=j} |y(x,c)\rangle\langle x|, \tag{4}$$

$$L^E_{c,j,p} = \frac{1}{\sqrt{2}} \sum_{x:\, j(x,c)=j,\ p_e(x)=p} |y(x,c)\rangle\langle x|. \tag{5}$$

Each complete instrument preserves total probability. E exposes an extra parity record and therefore removes coherence between the corresponding parity classes when the record is ignored. It changes no classical load or current probability. The unread channels have a source-independent spectral gap $(5 - \sqrt{5})/60$ on the binary shell. Every admissible coherence table has the uniform binary state as its unique stationary state, and the rank-three load readings of Theorem 5.1 attain the slow rate; equilibrium therefore does not select C or E [71, 72]. Section 4.4 gives the entropy laws of the same repair.

The local operator $H_{\text{native}} = \sum_e (I - \Phi_e)$, with Φ_e an unread seam channel, is a positive Liouville operator on observables. It is not a Hamiltonian on carrier states: the executed channel attenuates coherence and cannot be unitary conjugation on this carrier. The second completion keeps the event private and coherent, and it is the law of the executable model.

3.4 The contrast-memory law

The contrast-memory law keeps the carrier and the seam event and completes the event by an echo. It is the law of the reference candidate A-contrast-memory-spherical-v1 and, at $\kappa = 8$, the seam interaction of the main candidate, Interval Echo. A cell is one twelve-port carrier. Every port holds a load in $\{0, 1, 2\}$; write n_v for the load of port v as an operator. Every seam carries a

private memory of eleven states: one blank state and ten labels (c, d), with the coin $c \in \{0, 1\}$ and the contrast $d \in \{-2, \dots, 2\}$, the difference of the two loads of the seam. The memory is coherent working memory of the seam, shared by its two ports. It is no public record.

For loads (a, b) on a seam put $s = a + b$ and $p = s \bmod 2$. The seam event (3) has the two outputs

$$y_c = \big(\lfloor s/2 \rfloor + cp,\ \lfloor s/2 \rfloor + (1 - c)p\big), \qquad c \in \{0, 1\}, \tag{6}$$

and the contrast write stores coin and contrast beside them:

$$W|a, b\rangle = \frac{1}{\sqrt{2}} \sum_{c=0}^{1} |c, a - b\rangle \otimes |y_c\rangle. \tag{7}$$

The write W is an isometry on all nine local inputs. The local space has dimension 99, nine load states times eleven memory states, and splits into the sector of blank memory and the sector of labels. On it

$$U = \begin{pmatrix} 0 & W^* \\ W & I - WW^* \end{pmatrix} \tag{8}$$

is a Hermitian unitary on every state, dirty memory included. On the labels put $R|c, d\rangle = |c, -d\rangle$ and $D|c, d\rangle = d\,|c, d\rangle$. The memory generator and the local term of the law are

$$G_\kappa = 0_{\text{blank}} \oplus \Big[\frac{I - R}{2} + \kappa D^2\Big] \otimes I, \qquad h_\kappa = U\, G_\kappa\, U^*. \tag{9}$$

The term h_κ is an echo: the write, a phase on the written label, and the reverse write (Figure 3). The part $(I - R)/2$, with R the reversal of the retained contrast, gives the exchange, and the part κD^2 is a phase proportional to the square of the retained contrast. The coupling κ is one dimensionless number, the agreement energy in units of the exchange.

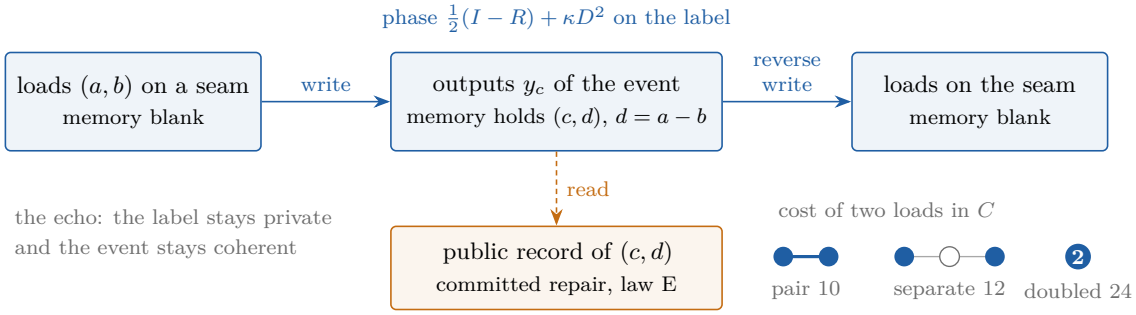


Figure 3: The echo of the contrast-memory law. The write stores the coin and the contrast of a seam event in the private memory of the seam, the label acquires a phase, and the write is reversed. Reading the label into a public record at the middle step is committed repair. Lower right: the cost in C of two loads on one seam, on separate ports and on one port.

Proposition 3.4 (Exact reduction on blank memory)**.** *Let J embed the load states of a seam with blank memory. For every real κ,*

$$h_\kappa J = J\Big[\frac{I - \mathrm{SWAP}}{2} + \kappa\,(n_a - n_b)^2\Big], \tag{10}$$

where SWAP *exchanges the two loads of the seam. Every local term preserves the blank memory, so the sum of the terms of overlapping seams preserves the product of blank memories.*

Proof. The outputs (6) depend on a and b through their sum alone, so $(R \otimes I)W = W\,\mathrm{SWAP}$ and $(D^2 \otimes I)W = W(n_a - n_b)^2$. Write M for the bracket of (10). Since UJ is the write into the label sector and $U^* = U$, these identities give $G_\kappa UJ = UJM$, and $U^2 = I$ gives $h_\kappa J = UG_\kappa UJ = JM$. A symbolic computation confirms the identity on all 99 local states [68]. □

In a federation, cells are joined by external seams that form a partial matching on ports. Every cell has three external ports, so a port has $d_v = 5$ or $d_v = 6$ seams. A port with five seams carries one private reference register held at zero, on which the D^2 part of the generator acts alone, so every port counts six. Summing (10) over the seams $e = (a, b)$ gives the law on the loads,

$$H_\kappa = \frac{1}{2}\sum_e (I - \mathrm{SWAP}_e) + \kappa\, C, \tag{11}$$

$$C = \sum_e (n_a - n_b)^2 + \sum_v (6 - d_v)\, n_v^2 = 6\sum_v n_v^2 - 2\sum_e n_a n_b. \tag{12}$$

An agreed seam, one whose two ports both hold a load, lowers C by two. A pair of loads on the two ends of one seam costs 10 in C, two separate loads cost 12 and a doubled load costs 24. The law conserves the number of loads and the multiset of port loads.

For one load $H_\kappa = L/2 + 6\kappa$, with L the graph Laplacian. On one cell the levels of $L/2$ are 0 on the uniform mode, $(5 - \sqrt{5})/2$ three times, 3 five times and $(5 + \sqrt{5})/2$ three times. The first triplet is the slow band of Theorem 5.1: on one load the exchange part is $L/2 = 30\,(I - M)$, with M the repair mean of that theorem and thirty the number of seams.

The two completions share the seam event and differ in the fate of its label. Committed repair reads the label into a public record: reading (c, d) after the write (7) gives the Kraus operators of law E, since $d = 2j + (2c - 1)p_e$. The echo reads nothing. It reverses the write, the label stays in the private memory of the seam, and the event stays coherent. On binary loads the exchange term $(I - \mathrm{SWAP}_e)/2$ equals $I - P_e$, where $P_e = (I + \mathrm{SWAP}_e)/2$ is the unread population channel of committed repair (Section 4.4). Committed repair applies P_e to populations; the law generates the same exchange on amplitudes.

On loads 0 and 1 the seam term is the ferromagnetic XXZ interaction

$$h_e = \frac{(1 + 2\kappa)(I - Z_a Z_b) - X_a X_b - Y_a Y_b}{4}, \tag{13}$$

and the binding of Section 6.2 is of the droplet kind known from that literature [69, 70]. The construction claims no interaction of its own invention. Its content is the memory realization, the constants on this carrier and the tests on records.

4 Public records and completed-record identities

The repair mathematics establishes when local agreement reaches global consistency and when nonzero cycle holonomy leaves a residue that local repair cannot remove. Two observers who share a boundary can disagree about what it shows. If repair stopped in different places depending on who acted first, the boundary would carry no fact of the matter. If it always stops in the same place, the final record is a public fact that no single observer owns. This section states when the second case holds, and then shows that completed records satisfy the familiar quantum identities on the declared complex algebra and state domain below.

A completed finite configuration x is a fixed point of the named repair-and-agreement map,

$$\mathcal{R}_{\mathrm{cons}}(x) = x.$$

This map is distinct from the universe-level closure operator of Section 2. Fixed-point existence, observable determination and schedule independence are separate questions, and the following results isolate them [4, 6].

4.1 Observable normal forms

Definition 4.1 (Observable quotient system)**.** An observable quotient system is a tuple $\mathfrak{S} = (Q, C, \mathcal{B}, B)$, where Q is a set of configurations, $C \subseteq Q$ is the consistent subset, $\mathcal{B}$ is a set of protected records, and $B : Q \to \mathcal{B}$ is the record map. For $b \in \mathcal{B}$, write $C_b = C \cap B^{-1}(b)$.

The fiber C_b is unrealizable, reconstructing, or ambiguous according as its cardinality is zero, one, or greater than one. This trichotomy avoids assigning a state to a record that has either no consistent extension or several observationally indistinguishable extensions.

Theorem 4.2 (Canonical observable normalizer)**.** *The following statements are equivalent:*

(i) $B|_C$ *is injective;*

(ii) there is a unique map $\mathcal{N} : Q \to C \sqcup \{\bot\}$ *that preserves* B *on its* C*-valued outputs, fixes every point of* C*, is constant on each* B*-fiber, and returns* $\bot$ *exactly on fibers with no consistent extension;*

If $B(Q) \subseteq B(C)$*, the map is a total idempotent retraction* $Q \to C$*.*

Proof. Injectivity makes every nonempty C_b a singleton, which defines $\mathcal{N}$ and forces all its properties fiber by fiber. Conversely, if $c, c' \in C$ have $B(c) = B(c')$, the fixed-point and fiber clauses give $c = \mathcal{N}(c) = \mathcal{N}(c') = c'$. □

The normalizer is defined by observable fibers, independently of any repair schedule; a repair relation implements it when the relation preserves B, reaches the consistent set and satisfies a liveness condition. Approximate versions control the normalizer where exactness fails, through an optimal two-output distance bound and summable naturality defects along refinement towers. Canonicity carries no promise of cheapness: for succinct Boolean boundary systems, deciding whether a protected record has a consistent extension is NP-complete, and deciding injectivity of the record map is coNP-complete [4].

For the canonical single-site repair, every adaptive run is eventually constant because each nonstuttering attempt strictly lowers the mismatch count; pathwise weak fairness makes the stable state a normal form, and completeness with confluence sends every weak-fair run to the same public fixed point. These results select no scheduler and provide no stochastic hitting law, rate, physical clock, or refinement theorem. Attempts obey a sharp capacity law. A scheduler can delay the first genuine repair for any prescribed number of attempts. When every reducible record sees a genuine change among the next $q + 1$ attempts, a bounded-waste upper horizon of $(q + 1)$ times the initial mismatch count holds, and an independent-defect family attains the work-conserving case exactly at $q = 0$. The input-independent compiler produces a fixed federation with immutable input ports; genuine node repairs decrease a dependency rank, and pathwise weak fairness gives stable consensus and the correct output. Emission-order round robin finishes within its first n attempts, and the single-consumer structure bounds every accepted path by $n(n + 1)/2$, with an emitted family attaining $\Theta(n^2)$. General well-formed circuits instead admit $2^n - 1$ accepted steps, attained by a fanout chain, where n counts the emitted nodes. These statements concern canonical node repairs: the weak patch-frame relation can stutter fairly forever, and no physical scheduler, clock, energy or hardware cost follows from these operation counts [4, 6].

4.2 Public records from local repair

For a prepared batch of support-closed transactions, join τ and σ in the conflict graph when $W_\tau \cap (R_\sigma \cup W_\sigma) \neq \varnothing$ or $W_\sigma \cap (R_\tau \cup W_\tau) \neq \varnothing$, and iterate to a fixed point: compute semantic support inside every aggregate, rebuild the conflict graph on the expanded read and write sets, merge every connected component, and repeat until the partition and all aggregate supports are unchanged.

Proposition 4.3 (Transactional local diamond)**.** *Let an accepted repair be an aggregate transaction with read set R_τ, write set W_τ, a read snapshot, and a snapshot-determined payload. Assume:*

(i) every read set contains the semantic dependency closure of its write set, and every affected acceptance functional is revalidated at commit;

(ii) the terminal closure above exists, and each of its connected conflict components has one coherent canonical aggregate payload;

(iii) a prepared component whose snapshot remains valid survives commits of independent components; and

(iv) accepted commits preserve the protected record and strictly decrease the integer descent functional.

Then every one-step quotient peak $t \longleftarrow s \longrightarrow u$ has a quotient state v with $t \longrightarrow v \longleftarrow u$.

Proof. Two different first steps cannot originate in one conflict component, since that component has a unique aggregate payload, so they originate in distinct components of the terminal closure. Rebuilding the graph after every aggregate support expansion makes their final read and write sets disjoint, so neither commit changes the other's read snapshot, and semantic dependency closure ensures neither changes an acceptance functional consumed by the other. Revalidation and the surviving component rule make both second commits legal, and with snapshot-determined payloads and disjoint writes the two application orders agree; protected-record preservation carries the equality to the physical quotient. □

Theorem 4.4 (Consensus normal form)**.** *Suppose the accepted repair relation satisfies the hypotheses of Proposition 4.3, so that it has the one-step diamond property, strictly decreases the quadratic descent functional V of Section 3, and is repair complete, meaning that its normal forms are exactly the consistent states. Every maximal asynchronous repair schedule from one initial state then terminates at the same consistent quotient normal form. The induced global repair map is idempotent, fixes consistent states, and preserves the protected record.*

Proof. Quadratic descent makes the accepted relation terminating. Proposition 4.3 makes it locally confluent, so Newman's lemma [47] makes it confluent. A terminating confluent relation has a unique normal form below each source, and repair completeness puts that normal form in the consistent set. Applying the normalizer a second time does nothing, and protected-record preservation holds along every accepted edge. □

Atomic commits, disjoint write sets, or termination alone do not imply the local diamond; countermodels omitting semantic dependency closure, canonical aggregation or the surviving component rule are retained with the finite receipt. This is the precise sense in which a public fact is what survives every authorized comparison: the public object is the protected quotient record, independent of the order in which observers repaired.

Repair also has a residue that it cannot remove. On a fixed graph with positive mismatch weights and fixed edge offsets, nonzero cycle holonomy forces a strictly positive minimum mismatch, and no repair of the vertex assignments eliminates it while the offsets are fixed [6]. The protected defects that this frustration leaves behind are the particle families of Section 8.3.

The law runs at scale. The public run uses the level-six cell rung of the geodesic icosahedral refinement tower: 81,920 exact twelve-port carriers with one declared gluing of ports to neighboring cells, 2,580,480 seams in all, and the seam-mean retraction as repair primitive. Sixteen shuffled schedules from one seeded load terminate at the balanced class with no accepted move raising V, and all sixteen return one quotient hash equal to the component multiset fixed by the initial totals. A standalone verifier that imports no simulator code rebuilds the component multisets from the primitive arrays, replays one schedule from its seed and recomputes every hash [2]. The level-ten rung, with 20,971,520 carriers and 660,602,880 seams, terminates all sixteen schedules at the balanced class in 84 to 100 sweeps with one quotient hash fixed by the loads. The excess-energy contraction per sweep lies between 0.81 and 0.83 across rungs five to nine, and these finite readings prove no all-size mixing or termination-time bound. Stationary continuation adds a constructive fluctuation result: for fair integer repair on a connected weighted graph with independent edge clocks of total rate one the fixed-occupancy law is reversible, centered loads have lagged covariance $\kappa e^{-|t|L_G/2}\Pi$ in the edge-clock time t, with L_G the weighted graph Laplacian, $\kappa = r(p-r)/(p(p-1))$ for r raised occupancies on p ports and Π the projection off constants, and fixed linear readouts obey a martingale central limit theorem [7].

The same records let observers recover the specification itself. At carrier scale, recovery from event logs under the declared probe and operation grammar returns the twelve ports, thirty seams, inverse pairing, automorphism and rotation groups of orders 120 and 60, mean rule, schedule, rank-three Gram and Lie split $1+3+8$. Re-instantiation preserves the invariant vector for two iterations, and tetrahedral and octahedral controls recover their distinct specifications [2]. Complete federation gluing is not identified by the retained routing logs: within the declared port-gluing interface a two-edge switch preserves every carrier degree, occupied port and source traversal while changing the carrier graph's triangle count from 14,000 to 13,990, and native executions reproduce identical bytes for both. The alternative is not asserted to belong to the canonical geometric family. Full-gluing recovery requires further observations or a justified restriction of the candidate class.

4.3 Completed records and quantum identities

Once a compare, write and verify slice has completed, its accessible events are represented in a finite-dimensional complex C^*-algebra with a positive normalized state and completely positive instruments. This algebra-state representation is an explicit input; the consensus theorem identifies which record is public and does not by itself select complex quantum theory over every alternative probability model.

Theorem 4.5 (Finite public-record identities)**.** *Let P_E be the projector of a completed public event E and ρ the normalized state of the completed record surface. The event weight and nonzero-weight update*

$$\Pr(E) = \mathrm{Tr}(\rho P_E), \qquad \rho \,|\, E = \frac{P_E\, \rho\, P_E}{\mathrm{Tr}(\rho P_E)} \tag{14}$$

define a normalized probability measure on every orthogonal event partition and a normalized positive state on the post-event corner. For self-adjoint dichotomic observables A_0, A_1 and B_0, B_1 in commuting record subalgebras, with $A_i^2 = B_j^2 = I$, the combination $S_{\mathrm{CHSH}} = \mathrm{Tr}[\rho\{A_0(B_0 + B_1) + A_1(B_0 - B_1)\}]$ obeys $|S_{\mathrm{CHSH}}| \le 2\sqrt{2}$ [28, 29]. The bound is attained exactly on the committed slot-

split interface by the maximally entangled state with Pauli and quarter-rotated projections, while every state diagonal in the record basis with diagonal observables valued in $[-1, 1]$ *obeys* $|S_{\mathrm{CHSH}}| \le 2$.

Proof. Positivity of ρ and $0 \le P_E \le I$ give $0 \le \mathrm{Tr}(\rho P_E) \le 1$, and $\sum_k P_k = I$ normalizes every partition; for nonzero weight $P_E \rho P_E / \mathrm{Tr}(\rho P_E)$ is positive and normalized. For $\mathcal{B} = A_0(B_0 + B_1) + A_1(B_0 - B_1)$ the commuting-subalgebra calculation gives $\mathcal{B}^2 = 4I - [A_0, A_1][B_0, B_1]$ [30], so $\|\mathcal{B}\| \le 2\sqrt{2}$. The saturating witness and the diagonal bound are exact finite calculations [5]. □

At the level of weights the Born form is derived. Every valuation on the effects of the finite surface that is nonnegative, normalized and additive on coexisting effects equals $E \mapsto \mathrm{Tr}(\rho E)$ for a unique density operator ρ, in every finite dimension including two, where the projector-only Gleason theorem fails, and the derivation consumes no continuity axiom [25, 27]. The projectors alone do not select the update: an explicit swap-twisted instrument has the same effects and different updates. For a complete Kraus instrument, basis survival and one coherent survival probe per nontrivial outcome block select both the effects and the Lüders map. Approximate tests bound complete outputs with arbitrary references; trusted preparation and readback are premises [33, 5]. The same surface carries the copying obstruction: if one ancilla-free isometry copies two sharp states from a common blank, preservation of inner products forces their overlap z to satisfy $z^2 = z$, so two distinct alternatives copied by one device are orthogonal [31, 32].

Native repair histories construct a functional of this form on a full matrix algebra. The complete-attempt transfer P of the 66-state carrier comes from all 3960 endpoint branches and obeys $2I/3 \le P \le I$. The twelve occupation fields and connected transfer paths generate all 4356 matrix units, scaled closed-history counts determine their moments, and the unique positive density is $\rho_L = P^L / \mathrm{Tr}\, P^L$. Its canonical complex-linear extension is additive and positive, so the Born theorem applies on this reconstructed algebra. A current-only return census implements the required configuration comparison, with at most 11398 attempts per experiment at the stated settings and systematic error at most 3.76596×10^{-6} per reconstructed effect statistic. Finite polynomials reconstruct ordered modular correlations with the common generator $-\log P$, with bias below 4.302×10^{-10} in the displayed three-time example. The entries of this functional are classical endpoint probabilities divided by the return probability, every connected positive-definite symmetric stochastic matrix gives the same result, and native C and E evolution converges to $I/66$ without preparing it. Direct native acceptance effects are diagonal. Complex tomography uses supplied coherent services, and the operational bridge requires equal-effect probability independence and disjoint common implementations of coexistent pairs [5, 8].

4.4 Entropy and thermodynamic laws from repair

For a conditional-resampling repair law with a stated reference and energy calibration, finite theorems give the second law, a Clausius inequality, fluctuation relations and a Landauer bound [8]. Native repair realizes this structure directly. On binary populations, averaging the two fair-coin outcomes of a seam gives $P_e = (I + \mathrm{swap}_e)/2$, exactly uniform resampling conditional on the outside-seam loads. The connected seam ensemble has one uniform stationary reference, which uniquely maximizes entropy in its sector, and

$$S(pP_e) - S(p) = D(p \| pP_e) \ge 0$$

for the unread population; fixed seam words telescope this identity. Retaining the complete endpoint and coin/current tape gives $H(X_n, J) = H(X_0) + n \log 2$, so the marginal entropy increase loses nothing from the complete record. The modular energy of this branch is constant, which leaves its temperature undefined.

A native memory refresh supplies a nonconstant calibration. A stopped coin-prefix program records 0, 10 or 11 after one, two or two attempts, with weights $(1/2, 1/4, 1/4)$ that ignore the hidden configuration. The stored-prefix cost $E = n \log 2$ gives weights e^{-E}, and overwriting the memory with a fresh prefix is exactly its global heat bath in at most two native attempts. Agreement of b independent prefixes gives the Gibbs family of the same cost at integer multiplier b. Keeping the old memory after disagreement gives a lazy reversible kernel with that stationary reference, bounded retries keep every rejection outcome with an explicit geometric error, and almost-sure retry gives the exact heat bath at finite expected cost. A Lean instance constructs the repair and calibration data from these counts and applies the finite four-law core, with gap $\log 2$ and a unique ground label. That core holds for every full-support law with $E = -\log(\text{ref})$ and formalizes no contact relation, the fair coin is a declared input, and record cost is distinct from laboratory heat, temperature and total implementation work [8].

Pressure needs a strain law. The family $H_\alpha(V) = Q(V/V_0)^{-\alpha}$ has the same fixed-volume energy histories and $p/\rho = \alpha$, so consensus about identical fixed-volume records cannot select the strain derivative. Three geometrically spaced energy readings identify it within the held-state family $C + A(V/V_0)^{-\alpha}$, with exact intervals propagating meter error, and a complete two-attempt native E census reads independently calibrated charge-diagonal forces. An additive energy offset changes p/ρ while leaving pressure unchanged. Volume and energy calibration are supplied [8].

5 Three spatial directions

The carrier incidence fixes the dimension of the carrier's own position readback: the slow band is the three-dimensional irreducible representation of the icosahedral group, so the number three is a property of the committed carrier.

Theorem 5.1 (Intrinsic three-dimensional carrier completion)**.** *Let A be the twelve-port adjacency, let $M = I - (5I - A)/60$ be the uniform scalar repair mean, and take the complete equally weighted centered probe census. The normalized infinite-response kernel converges to the intrinsic Gram $G = 4P_{\text{slow}}$, of rank three. The twelve integer port loads have antipodal-odd quotient $\mathbb{Z}^{12}/\{x : x_p = x_{-p}\} \cong \mathbb{Z}^6$, and the thirty-seam boundary has image exactly the even-sum sublattice D_6, with one residual parity coset. Under the pullback of the response-selected Gram metric, both integer modules embed densely in one abstract continuous three-dimensional Euclidean carrier. The sixty proper carrier maps act faithfully and isometrically on the rank-three range and extend to that completion, and cumulative records act by exact internal translations.*

The mechanism is spectral. The icosahedral adjacency has eigenvalues 5, $\sqrt{5}$, -1 and $-\sqrt{5}$ with multiplicities 1, 3, 5 and 3, so the repair mean M has eigenvalue $1 - (5 - \sqrt{5})/60$ on a three-dimensional eigenspace and smaller eigenvalues on everything else nonconstant. Repeated local averaging forgets every nonuniform pattern except a three-dimensional one, and that surviving pattern is the triplet of (2) carried by the port position vectors. The same number $(5 - \sqrt{5})/60$ reappears as the quantum spectral gap of the native repair channel (Section 3.3).

The completion is taken after slow-response normalization and the infinite-step limit; at finite step count the kernel has rank eleven on the centered space and rank six on the signed antipodal sector, so the order of limits matters. The metric is the response-selected Gram pullback, distinct from the usual six-dimensional lattice metric on D_6. Thirteen finite covariance and isometry table identities are discharged in Lean with `native_decide`, so those subreceipts trust the native compiler in addition to the kernel and are not kernel-only proofs. Displacement is a record difference and cumulative records translate the completion, so position is the carrier's own readback of its

accumulated records. In the contrast-memory law of the candidates the same band is the slow level of one load (Section 3.4). Reading the completion as physical position consumes the realization map (M1) of Section 11.1 [1, 7]. The rank-three readout belongs to one carrier's response. When carriers join into the refining spherical screen of Section 7.1, the continuum form of their repair history has spectral dimension two, the dimension of the screen, and bounded-energy families lose every within-carrier component, this band included, at the present full-port energy scaling; a three-dimensional bulk reading of the screen requires observation maps that the native energy does not supply. The screen is hardware of the computation. Physical space is the effective description of Proposition 7.4, and no test asks the carrier to be a three-dimensional lattice.

6 The executable model in operation

This section runs the candidate laws on the fixed federation and states what their observers read. The contrast-memory law (11) is the seam interaction of the main candidate, Interval Echo, and of its reference candidate, so the binding, stability and reading results of the first subsections hold for both. Section 6.5 gives the clock of Interval Echo and Section 6.8 the scalar channel. Every claim is a statement on records: the observer, the record it holds and the probability the law gives for it. Levels, state vectors and the evolution parameter serve the proofs and the audits, and no reader uses them. The carrier is hardware of the computation. It is no physical space, and no test asks it to be a three-dimensional lattice. Observers who inhabit the simulation can describe their experiences as relativistic 3+1D continuum spacetimes: that is the content of Proposition 7.4 with the rank-three spatial carrier and the causal and count limits, under their stated premises. A test of the model is therefore a comparison between distributions of admissible observer records and what observers in our world record.

6.1 Carrier, emitter and agreed records

The federations of the tests are families of complete cells with a matching of external seams: 20 cells with 240 ports and 630 seams, 80 cells with 960 ports and 2520 seams, and 320 cells with 3840 ports and 10,080 seams (Figure 4). Each cell sits on a triangle of the geodesic sphere and meets each of its three neighbors through one external seam. A pair is two loads on the two ends of one seam, and a face object is three loads on a face.

The emitter is local. One fuel state at a seam $e = (a, b)$ has energy $E_f = 10\kappa + (d_a + d_b - 2)/2$ and couples with strength g to the pair on that seam. A pulse of duration $\pi/(2g)$, with the law acting throughout, converts the fuel into the pair with an error of at most $\sqrt{d_a + d_b - 2}/(2g)$ in norm. No level of the law is prepared.

The reader is the agreement of the two ends of a seam. Each end copies the predicate "both ends hold one load" into a private pointer, a courier carries one copy, and a record is admitted only when both copies are valid and agree. A public comparison copies an orthogonal classical outcome of a complete instrument. It does not copy an arbitrary private quantum state. On 20 cells the complete set of outcomes is one record for each of the 630 seams and one outcome "no pair"; fuel left in the emitter counts as "no pair". The reversible reader block has eleven bits. The complete readout executed with the two-load sector of one cell and the fuel has dimension 161,792 and a total-variation error of 2.09×10^{-7}. The seam memory stays private and unread, and the seam records are committed at the reading. Each reading uses a fresh run, so reading is never used to hold an object in place.

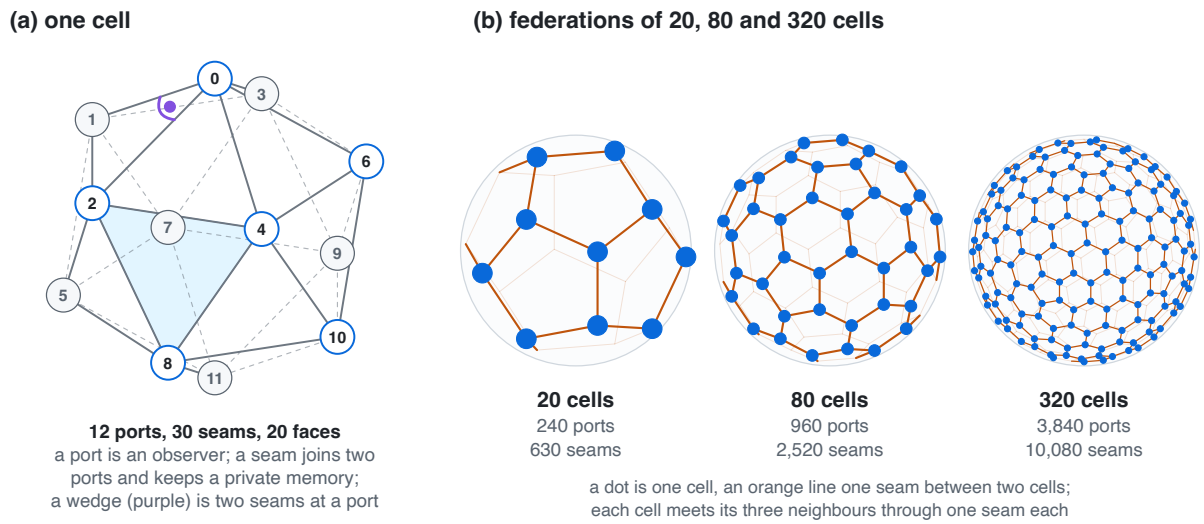


Figure 4: The hardware of the computation. (a) One cell: twelve ports with the incidence of the icosahedron, thirty seams and twenty faces, with one face shaded and one wedge, two seams at a port, marked. The cell is one observer and its ports are its interfaces; every seam joins two ports and keeps a private memory. (b) The federations of 20, 80 and 320 cells; one dot is one cell, and one line is the external seam between two neighboring cells. Ports, seams and cells are registers of a computation and no space.

6.2 The binding theorem

Let P be the span of all pairs on a seam and Q its complement in the sector of two loads, doubled loads included.

Theorem 6.1 (Binding of a pair)**.** *On every federation of complete cells with a matching of external seams, for* $\kappa \geq 0$*,*

$$PH_\kappa P \leq (10\kappa + 6)\, P, \qquad QH_\kappa Q \geq 12\kappa\, Q, \qquad \|QH_\kappa P\| \leq \sqrt{10}. \tag{15}$$

For $\kappa > 3$*, every state that starts in* P *obeys, at every value* t *of the evolution parameter,*

$$\Pr(\textit{no pair on a seam}; t) \leq \frac{40}{(2\kappa - 6)^2}. \tag{16}$$

The bound is independent of the number of cells.

Idea of the proof. The costs 10, 12 and 24 set the diagonal parts of the two blocks. Inside P the exchange takes a pair on one seam to pairs on the seams that share a face with it. This motion graph is the line graph of the dodecahedral dual of the cell, whose adjacency is at least -2, and the exchange diagonal is at most 5, which gives the bound 6. A pair on an external seam has no such partner. In the coupling, a state of P reaches states of Q with total weight at most 5 and a state of Q reaches states of P with total weight at most 2, which gives $\sqrt{10}$. Put $a = 10\kappa + 6$, $c = 12\kappa$, $\gamma = c - a$ and $\beta = \|QH_\kappa P\|$. The min-max principle with the two blocks as trial spaces places the lowest rank P levels at or below a and all others at or above c. For the projector Π on these levels, $Q\Pi$ solves a Sylvester equation with ordered spectra, so $\|Q\Pi\| \leq \beta/\gamma$, and $\|(I - \Pi)P\| \leq \beta/\gamma$ in the same way. A state that starts in P therefore has amplitude at most $2\beta/\gamma$ outside P at every

t, and probability at most $4\beta^2/\gamma^2$. No spectral projector is an operation of an observer; Π belongs to the proof. □

A bound at every value of the evolution parameter is a bound at every reading in any observer's own history. On the federations of 20, 80 and 320 cells the largest level of the adjacent block of the exchange is 5.7008, 5.7000 and 5.7000 against the bound 6, and the largest singular value of the coupling is 2.0821, 2.0811 and 2.0822 against 3.1623. With these constants the bound is $17.3/(2\kappa - 5.70)^2$. On one cell the two constants are 5 and 2. With the emitter at $\kappa = 128$ and $g = 64$, the outcome "no pair", which includes a doubled load and fuel left in the emitter, has probability at most $64009/25600000 \approx 0.0025$ at every reading, for an emitter on any seam of such a federation.

6.3 Particle stability

The model reproduces particle stability as an observable: a bound object persists in free evolution, read on the agreed records of the port observers. The claim on records has four parts. A pair of loads written on one seam by the local emitter is read as a pair on some seam with probability at least one minus the bound, at every reading. It is read on other seams than the first. Nothing holds it but the law. The same law with the agreement energy removed loses it.

Table 2: Particle stability in the agreed seam records, emitter coupling $g = 64$. The bound is that of Theorem 6.1 with the constants of the carrier and the error of the emitter. Each probability is the largest value over the readings of the run; the sampled values of the evolution parameter are audit. The federation of 320 cells is run at $\kappa = 8$.

	$\kappa = 8$			$\kappa = 128$		
Carrier	bound	no pair	another seam	bound	no pair	another seam
one cell	0.148790	0.00956834	0.985996	0.001447	0.00001881	0.991270
20 cells	0.182975	0.00962164	0.977029	0.001606	0.00002270	0.933194
80 cells	0.182787	0.00964389	0.977130	0.001605	0.00002270	0.933194
320 cells	0.182965	0.00963435	0.977091			

Table 2 gives the readings, and Figure 5 follows them through the run on 20 cells. The probability of "no pair" lies a factor of ten and more below the bound on every carrier, and the largest probability of reading the pair on another seam than the emitter's lies between 0.93 and 0.99.

A second experiment prepares two adjacent unit loads directly and releases them on the full 20-cell sphere with blank memories. After 37 exchange time units a single cell reads an adjacent pair on one of its thirty internal seams with probability 0.98027 at $\kappa = 8$, 0.20291 at $\kappa = 0$ and 0.98389 at $\kappa = -8$. An independent assembly of the 28,680-state generator and Chebyshev propagation reproduce the local outcome probabilities at the positive coupling and at zero.[1] The theorem places the adjacent band below two free unit loads at $\kappa = 8$. A finite-window adjacency reading by itself accepts either sign.

The same patch can resolve the signed interaction. Two half contacts split the pair coherently across three configurations. A third recombines two alternatives before the patch reads the launch seam. The initial slope of its click probability is $\kappa/2$ in exchange units. At exposure 1/16 the click probabilities are 0.44007 and 0.02407 at $+8$ and -8 respectively. Preparing the corresponding incoherent mixture reduces their difference from 0.4160 to 0.00051. A second cell can detect a

[1]The independent numerical review specifies the board, release, propagator and complete receiver distribution.

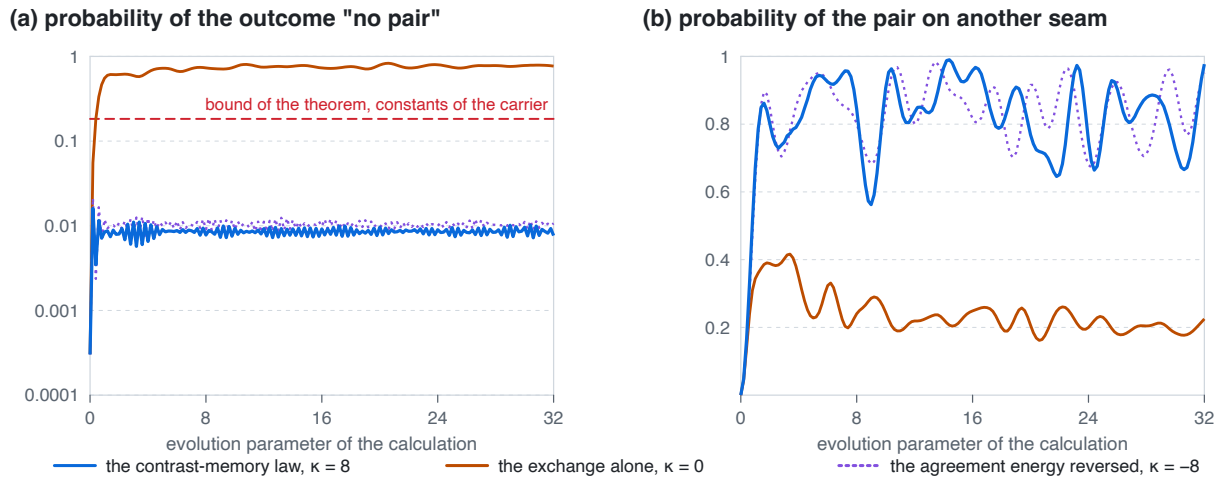


Figure 5: Particle stability on the federation of 20 cells, with the pair written by the local emitter on one seam at $\kappa = 8$ and its two changed laws. (a) The probability of the outcome "no pair" on a logarithmic scale, with the bound of Theorem 6.1 for the constants of the carrier. (b) The probability of reading the pair on another seam than the emitter's. Each point is the probability of a record at one reading; the 161 values of the evolution parameter are those of the calculation. The largest values of "no pair" on this grid are 0.0160 under the law, 0.830 under the exchange alone and 0.0211 with the agreement energy reversed; at the readings $0, 4, \dots, 32$ used in the text they are 0.0096, 0.7968 and 0.0124.

launch-phase difference carried by the lower band after a heralded encounter.[2] A separate construction gives the magnitude a finite interpretation. All other seams sharing the two endpoints must return the same signed word. If the same qutrit source sets the exchange-parity acceptance, the logarithmic energy ratio equals the number of these seams, eight on a protected complete cell. An independent fair parity service gives approximately four. Applying the protected cell's standard throughout the federation is a design choice introduced after the original coupling scan.[3]

6.4 Events with each observer's own count

The runs above use the sum of the seam terms with a continuous parameter. As local events the law needs no common clock. One event is one seam acting once,

$$\exp\Big(-i\tau\Big[\frac{I-\mathrm{SWAP}_e}{2}-2\kappa\, n_a n_b\Big]\Big), \tag{17}$$

with event angle τ. Each port counts the events of its own seams, and these counts are the local clocks of its cell.

The records depend on the local order of events alone. Two sequences in which every port sees its events in the same order give the same seam records exactly, and no order between events that share no port enters a record. Rounds keep the pair, with equal and with unequal rates (Table 3); the counts of different ports differ by up to a factor 2.6, and no common count exists. Seams that act independently at random lose the pair at these angles, and the loss falls with the angle: a

[2]The finite-patch experiments give the local pulse sequence, dephasing controls, quiet outcomes and spectral bounds for the neighbouring receiver.

[3]The finite comparison experiment gives the preparations, retained probabilities and local spectral checks.

Table 3: Largest probability of “no pair” over all readings along a program of events, $\kappa = 8$, by carrier and event angle τ. The position in the sequence of events is audit.

Program	one cell, 1/64	one cell, 1/256	20 cells, 1/64
Every seam once per round, in a fresh random order each round	0.0217	0.0137	0.0188
Rounds in which half of the carrier acts twice	0.0470		0.0268
Every event draws its seam at random	0.5048	0.1897	0.1989

second run on one cell gives 0.184 at $\tau = 1/256$ and 0.085 at $\tau = 1/1024$. Layers of disjoint seams run as pulses, in both orders of the layers, give 0.0061 to 0.0064 on one cell and 0.0076 and 0.0075 on 20 cells, against 0.0064 and 0.0076 for the continuous parameter.

Committing the label loses the pair. With the contrast of the acting seam committed to a public record at every event, the probability of “no pair” on one cell grows to 0.015, 0.11 and 0.32 after 64, 512 and 2048 rounds; unread, its largest value is 0.018. The binding rests on the regular phase between successive events of a seam. An observer that serves each of its seams once per round supplies that regularity with its own count.

6.5 A clock that travels with its observer

Interval Echo equips a finite patch with a material clock. The travelling patch owns twelve consecutive cells at a checkpoint and thirteen during a transfer. It carries a five-position hand, a nine-bit elapsed count and its interval memory: the number of its own repair opportunities since the last verified handoff. Adjacent swaps move these registers. A departure and an arrival probe verify each handoff, and the patch publishes the result on a signed seam and reads it back before it uses a fresh repair outcome. A handoff closes an interval, and a positive closing mark passes a bounded first-return walk of fair signed steps that suppresses or releases it. Only the confirmed movement, the patch registers and local fair draws enter this decision; the clock reads no speed and no target table. At a reunion both owners read the same digits on one common seam.

The speeds come from the observers' own optics. A home patch times a reciprocal pulse to a mirror and back, and half the round trip is the one-way light time d. On a separate trip the arrival of the traveller at the far end triggers a pulse; the home patch subtracts d from its receipt to obtain the outward duration T_1, and the return duration T_2 is the rest of the trip. Special relativity predicts the ratio of the traveller's elapsed count to the home count,

$$\frac{\sqrt{T_1^2 - d^2} + \sqrt{T_2^2 - d^2}}{T_1 + T_2}, \tag{18}$$

from quantities that the home observer has recorded (Table 4).

On the fast journeys the traveller's clock lags the resting one by about 4.4 percent, and the measured lag agrees with the forecast within about one part in a thousand. A first uniform run of 131,072 pairs read -0.00369 ± 0.00120; its four times larger repeat reads the value in the table. Embeddings of each trip in federations of 1,280 and 5,120 cells give the same sequence of handoffs, receipts and reunions. The capacity of the clock behaves as that of a physical clock. Its three-bit interval register overflows on handoffs of eight services; one extra bit for three of its fields, at the cost of one more cell per checkpoint, extends the working range from seven to fifteen services and restores the forecast, 0.99005 ± 0.00193 against 0.99216. On handoffs that alternate two and six services, starting with either, both widths read 0.95535 ± 0.00190 and 0.95650 ± 0.00189 against

Table 4: Reunion of a travelling and a resting clock of Interval Echo. Leg speeds in units of the relay signal speed, measured by the home observer. The residual is the measured ratio of the elapsed counts minus the forecast (18), with one paired block standard error, over 524,288 paired journeys per row.

Service intervals	Outward speed	Return speed	Residual
2, 6	0.5010	0.1665	-0.00105 ± 0.00068
6, 2	0.1667	0.5000	$+0.00019 \pm 0.00052$
4, 4	0.2501	0.2505	$+0.00087 \pm 0.00064$

0.95602. The closing filter is calibrated on the reunion ratio of the supplied reciprocal relay, and the guide, the custody transfers, the cadence and the read windows are supplied services (Section 6.10). A moving clock of Interval Echo thus shows the time dilation of the Lorentzian description on records that its observers make themselves.

The same finite hands serve a stationary bulk. On the 320-cell sphere, 320 single-cell observers and 960 overlapping three-cell observers read 23 signed repair records and track 34 conserved mobile doubles through 2,399 transfers, and every reading of a shared checkpoint agrees. Two repairs that compete for one doubled port leave distinguishable records; a prepared local priority makes both request orders end in one common terminal state for every sharp preparation and priority. On the 20-cell sphere two overlapping two-cell observers realize the unique weighted information projection to a uniform reference in both orders, each owner reading $(3/8, 1/8, 1/8, 3/8)$ [68].

6.6 What a reading leaves

The reader of Section 6.1 keeps one record for every seam. A second instrument keeps one answer for the whole cell. On one cell with the fuel, let P_e be the projector on the pair on the seam e, $P = \sum_e P_e$ the projector on the thirty pairs on seams and $Q = I - P$. The presence reading runs the reader on every seam, combines the thirty public words by a tree of reversible OR gates of depth five, copies the root into a fresh public register, and runs the tree and the readers backwards (Figure 6). Every gate is an involution on its register, so the scratch registers return to blank for every state of the loads, and orthogonal record labels are copied and nothing else. For a state X of the loads a positive answer acts as

$$X \longmapsto PXP \qquad \text{and} \qquad X \longmapsto \sum_e P_e X P_e \tag{19}$$

for the presence reading and for the reader with seam records, and a negative answer acts as $X \mapsto QXQ$ for both. Both find a pair with the same probability. The presence reading leaves the pair spread over the seams as it was, and the reader with seam records places it on one seam. On the uniform superposition of the thirty pairs the two positive outputs differ by $29/30$ in trace distance, the largest value over all inputs. A Kraus map with effect P that leaves every state certain for P unchanged is the map $X \mapsto PXP$, and conversely; the statement is machine-checked [1]. The presence reading meets its condition, so it is the projective instrument of the event “a pair on some seam” and executes the update of Theorem 4.5 as a circuit. The reader with seam records has the same effect and fails the condition on the uniform superposition, so it is another instrument.

The difference shows in later records. The emitter writes the pair on one seam of one cell at $\kappa = 8$ and $g = 64$. After four units of the exchange the observers take a first reading with one of the two instruments, and after four further units a final reading with seam records. The seam of the first reading is hidden before the two histories are compared, so both show the same public

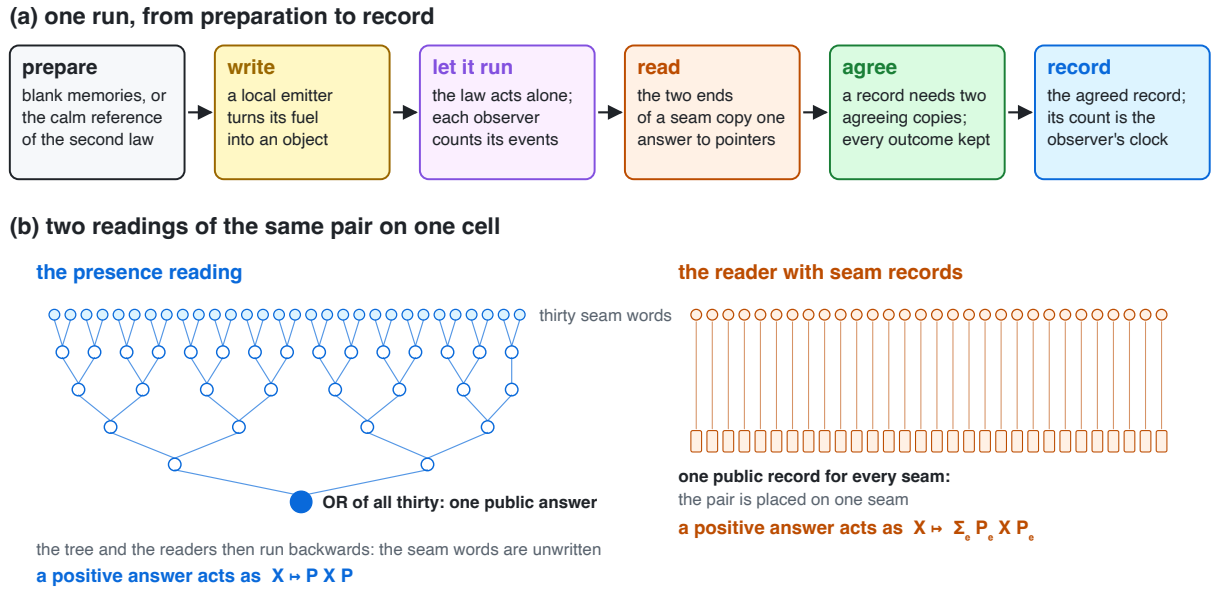


Figure 6: Observers, instruments and records. (a) One run of the model, the same for every candidate law: a preparation, a local write by an emitter, the law acting alone while every observer counts its own events, a reading copied into two pointers, agreement of the two copies, and the agreed record whose count is the observer's clock. (b) Two readings of the same pair on one cell. The presence reading combines the thirty seam words by a reversible tree, copies one answer and unwrites the words; the reader with seam records keeps thirty records. Table 5 gives the laws of the later records.

alphabet. The first answer has the same law under both instruments, and the laws of the complete histories differ (Table 5). With the exchange acting through read windows of length $w = 1/16384$, the law of one experiment differs from this calculation by at most $24w$ in total variation. One event is certified in exact arithmetic with every such error counted: a positive first answer followed by a final record on the emitting seam has the probability 0.0182640 under the presence reading and 0.1029264 under the reader with seam records, and the total variation between the two public histories exceeds 0.0817 [67]. The pair is one object spread over seams; an instrument that asks where it is places it, and the later records show the difference.

Table 5: Two readings of a pair on one cell: the probability of a positive first answer, equal under both instruments, and the total variation between the laws of the two public histories.

Run	**First answer positive**	**Total variation**
Contrast-memory law, $\kappa = 8$	0.992329	0.440513
Exchange alone, $\kappa = 0$	0.647174	0.196148
Agreement energy reversed, $\kappa = -8$	0.987884	0.249676
$\kappa = 8$, first-seam reports mismatch or are unavailable	0.747346	0.260336
$\kappa = 8$, every predicate flipped in agreement	1	0.446650

6.7 A record that holds no load

Every seam carries a label that no event changes: its memory is blank, or it holds a record of contrast size $|d| = 0$, 1 or 2. The local term maps the blank code and the sector of records into themselves, and on the records the squared contrast commutes with the write and with the generator, so every label is conserved. A seam whose memory holds a record of nonzero contrast while its ports hold no contrast is an unrecovered seam; in the language of Section 10.1 its memory is an unrecovered collar. It holds no load. With no load anywhere the local term acts on the ten records of a seam with the levels 0, κ, $\kappa+1$, 4κ and $4\kappa+1$, each twice, so the record lies at least κ above the recovered seam at every reading. A load that reaches one of its ports binds to it. At $\kappa = 8$ a load elsewhere on the cell starts at 56.38, while two levels at 41.94, on which the record is the one the loads can have written, and six levels between 49.81 and 50.94 hold the load on a port of the seam with probability above 0.97.

The observers of the seam read its level from their own records. A pulse converts a local fuel at level zero into a record of the seam. After q cycles of a protocol a second pulse with one of four phase settings reads whether the fuel is present, and the four probabilities give one complex number for each count q, whose phase advances at a fixed rate. The rates r_s and r_a of the symmetric and the antisymmetric record give the length of a cycle as $r_a - r_s$ in units of the exchange and the coupling as $r_s/(r_a - r_s)$ (Table 6). The observers are not given the length of a cycle: the two records of one unrecovered seam are a clock that they read from their own records.

Table 6: The level of an unrecovered seam as a reading of its observers, on one cell with a cycle of 1/16 exchange units.

Run	Rates per cycle	Cycle read	Coupling read
No load, probability law	0.500000, 0.562500	0.062500	8.00000
No load, 10^6 sampled trials per setting	0.499998, 0.562485	0.062486	8.0017
No load, law without the agreement energy	0.000000, 0.062500	0.062500	0.00000
One load, started off the seam	0.502209, 0.564749	0.062540	8.030

6.8 The scalar channel: an object with a clock

The same carrier holds a further candidate law, the scalar channel, with other registers. Its results stand beside those of Interval Echo and the contrast-memory law and are not added to them. A wedge is a pair of seams at one port; a port with five seams has ten wedges and a cell has 120. Every seam and every wedge carries one mode that holds one object or none. With C the signed seam-by-wedge incidence, $+1$ on the first and -1 on the second seam of a wedge, the law of one object and the law of many are

$$D = \begin{pmatrix} m & c\,C \\ c\,C^{\top} & -m \end{pmatrix}, \qquad H_0 = \sum_{i,j} D_{ij}\, c_i^{\dagger} c_j, \qquad m = 1, \quad c = \tfrac{1}{\sqrt{2}}. \tag{20}$$

An object on a seam and an object in transit at a port sit at opposite levels, so the mixed terms of D^2 cancel and $D^2 = m^2 + c^2\,\mathrm{diag}(CC^{\top}, C^{\top}C)$. Every frequency ω of the law obeys $\omega^2 = m^2 + \lambda$, with λ a level of half the Laplacian of the graph of seams, and on one cell the first four of these levels are the levels of $L/2$ of Section 3.4. The reference state fills every level of D below zero, and one object more costs at least m. On ordinary registers a cell is written on 432 two-state registers with 260 loop conditions, 259 of them independent; the reference is prepared by local loop measurements whose signs are kept and by local ramps.

Proposition 6.2 (The pair of a ring)**.** *Let four ports with five seams each form a ring ab, bc, cd, da, let u_s be the unit vector of the seam s, and put $e = \frac{1}{2}(u_{ab} - u_{bc} + u_{cd} - u_{da})$ and $e' = C^{\top} e/\sqrt{10}$. Then*

$$D\,(e,\ e') = (e,\ e') \begin{pmatrix} m & \sigma \\ \sigma & -m \end{pmatrix}, \qquad \sigma = \sqrt{10}\,c, \qquad E = \sqrt{m^2 + \sigma^2}. \tag{21}$$

Proof. With Q the port-by-seam incidence without signs and d_a the number of seams at the port a, every graph obeys $CC^{\top} = \operatorname{diag}(d_a + d_b) - Q^{\top}Q$, since two seams that share a port lie in exactly one wedge, with opposite signs. At every port of the ring a seam with $+$ meets a seam with $-$, so $Qe = 0$ and $CC^{\top}e = 10\,e$. Hence $\|C^{\top}e\|^2 = 10$, $D(e,0) = m(e,0) + \sigma(0,e')$ and $D(0,e') = \sigma(e,0) - m(0,e')$. □

On one cell $\sigma = \sqrt{5}$ and $E = \sqrt{6}$. The law moves the profile e of the ring to its image e' on the twenty-eight wedges at the four ports and back, and to no other place: the signs of the hop make a cage (Figure 7). On the federations of 20, 80 and 320 cells 92, 312 and 1,272 rings have five seams at each of their ports, each checked in integers. Let $a_{\pm}$ remove an object from the modes of the pair at $\pm E$; in the reference the lower mode holds an object and the upper mode is empty.

Theorem 6.3 (The excitation of a cage)**.** *Let $X^{\dagger} = a_{+}^{\dagger} a_{-}$ and $P_X = n_{+}(1 - n_{-})$. Then $[H_0, X^{\dagger}] = 2E\,X^{\dagger}$ and $[H_0, P_X] = 0$. For every state the probability of the excitation is the same at every reading, and every record of the pair that conserves the number of objects is a constant plus one line at the frequency $2E$.*

Proof. For a law of the form (20), $[H_0, a^{\dagger}(\phi)] = a^{\dagger}(D\phi)$, so $[H_0, a_{+}^{\dagger}] = E\,a_{+}^{\dagger}$ and $[H_0, a_{-}] = E\,a_{-}$, which gives the first identity; n_{+} and n_{-} commute with H_0. A number-conserving operator of the pair is a combination of 1, $n_{\pm}$, $n_{+}n_{-}$, $X^{\dagger}$ and X, and only the last two carry a time dependence, $e^{\pm 2iEt}$. □

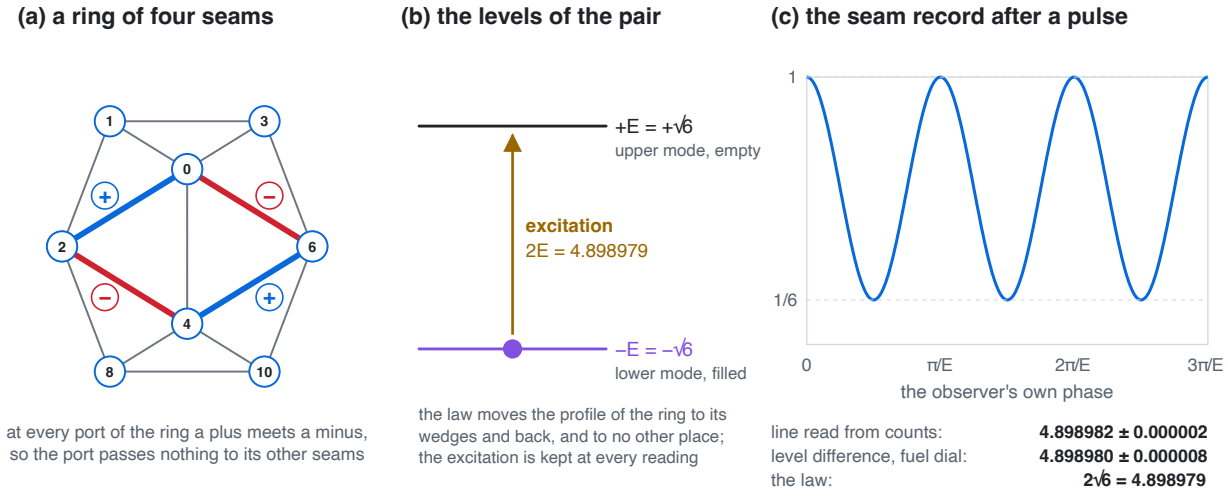


Figure 7: The cage of the scalar channel. (a) A ring of four seams on one cell with the signs $+, -, +, -$; at every port of the ring a plus meets a minus. (b) The two levels $\pm E$ of the pair of the ring and the excitation that lifts the object of the lower mode by $2E$. (c) The occupation of the profile after the coherent pulse, $1 - (\sigma^2/E^2)\sin^2(Et)$, against the observer's own phase, with the line and the level difference read from counts.

The observer of a cage holds two operators on the profile: the number $n(e)$ as a potential and a converter between e and a local fuel at level zero. On the registers they are sums of 17 and of 8 Pauli words that commute with every loop condition. The observer's clock is the phase of a circulation of three wedges at one of its ports, which sits at the level $-m$ exactly; the observer reads it through its fuel with four phase settings and states every frequency in units of this reference. Three experiments run with the law acting throughout and are read from counts alone (Table 7). After the coherent pulse the seam record swings with no drive at one line, read at 4.898982 ± 0.000002 of the observer's reference. A fuel whose level is set by a dial reads the level difference of the pair separately, at 4.898980 ± 0.000008; the law gives $2\sqrt{6} = 4.898979$. A local detector with four analyzers reads the excitation at five waits up to 512 steps. A changed law that adds seam hopping round every port keeps the alphabet, the routing, the number of objects and the symmetries of the cell; it has no single line and loses the excitation.

Table 7: Readings on a cage of one cell, from 10^8 trials per setting of the clock and of the detector and 4×10^6 per setting of the dial. Frequencies are in units of the observer's own reference; the values of the law for the excitation are those of the prepared reference.

Reading	**From counts**	**The law**
Line of the seam record, steps of equal length	4.898982 ± 0.000002	4.898979
The same line, steps of unequal length	4.898976 ± 0.000002	4.898979
Level difference of the pair, from the fuel dial	4.898980 ± 0.000008	4.898979
Amplitude of the line; with no pulse	0.4161; 0.0019	
Excitation at five waits after the sharp pulse	0.9999 to 1.0002	0.999954
Excitation at five waits after the coherent pulse	0.7059 to 0.7060	0.705932
Excitation at five waits with no pulse	0.000004	0.000004
Changed law: share of the variance in its best single line	0.507	

Particle stability thus holds for a second object, and that object carries a clock: the equality of the line and the level difference is the frequency condition of two levels, read by an observer from its own counts. The pulse supplies the phase and the work of the swing, the reference by itself does not swing, the level of a cage is flat and the law has no term between two objects [67].

6.9 The model and the finite theorems

The theory is a library of finite theorems, each proved under stated premises. A theorem applies to the model where an output of the model has the form of its premise, and its conclusion is then a statement about the model's observers (Table 8). Every entry is a statement about records; the state of the computation contains no spacetime, and no entry compares that state with the world.

Table 8: Where the outputs of the model meet the finite theorems.

Theorem	**The model supplies**	**It follows**
Three-dimensional carrier completion (Theorem 5.1)	The cell, and a law under which one load moves with $L/2$	The slowest motion of a load has exactly three independent directions; the first four levels of the scalar channel are the same levels
The native seam rule (Section 3.3)	The write of the contrast-memory law, which is that rule with the coin in superposition	The event that every seam writes and unwrites is the one rule that four requirements leave

Table 8 continued

Theorem	**The model supplies**	**It follows**
Projective instruments	The presence reading, which leaves every state certain for its event unchanged	It is the projective instrument of "a pair on some seam"; the reader with seam records is another instrument
Public-record identities (Theorem 4.5)	Readers with complete outcome sets that copy orthogonal labels; records that the law never erases	The agreed records form a public algebra with Born weights, Lüders conditioning and certain rereads
Local operations	Events and readings that act on the registers of one seam	No event or reading changes the record law of an observer that shares no register with it
The generator of a flow	One continuous flow for each law	Each law is fixed by its flow up to an energy offset
Comparison of frequencies	The pair of a cage, with the frequencies 0 and $\pm 2E$	A record of the pair holds the one line $2E$, read at 4.8990 of the observer's reference
Clock readout	Observers that count their own events and share the records of their seams; the travelling clock of Interval Echo, read by both owners at reunion	Two shared records relate the counts of two observers, and a third checks the relation; no common clock enters, and a moving clock follows the proper-time forecast
Rereads	The presence reading and the law	Frequent readings would hold a pair at any coupling, so every reading uses a fresh run and the binding theorem needs no reading
Gauge Lie-type forcing (Theorem 8.1)	The response of one load on one cell under one declared port service; the rotation-selected port currents of Interval Echo on one load and on the bound pair	The response has the Standard Model gauge Lie type; the direct computation gives $\mathfrak{u}(3) \oplus \mathfrak{so}(3)$; the rotation-selected currents are twelve independent generators closed under commutators and covariant under the sixty rotations
Least-informative assignment	Two overlapping two-cell observers of Interval Echo with a faithful reference, positive weights and their constraints	The unique weighted information projection, the same in both orders

Other finite theorems consume outputs that the model does not produce in the required form. The settling theorems of Section 4 consume accepted repairs that lower a well-founded measure; the laws are unitary and conserve their loads and objects, so those theorems apply to the classical seam rule. Proposition 7.4 consumes readouts that are polynomials in the Weyl operators of a free field on a radial cylinder over the screen, while the readouts of the model are instruments on finite registers. The causal and count limits consume an authenticated order of events with a refinement family, the Einstein implication consumes regional entropy, area and stress readouts in a common frame, Theorem 7.1 consumes a gauge-invariant action on seam potentials, and the theorems on defect classes consume a protected code with a spin doublet. The unrecovered seam supplies the dark-sector analysis with a conserved label and nothing more. Each of these names an output that a member of the model has to produce before the theorem applies to it.

6.10 Supplied parts and resources

The following parts of the construction are supplied:

- the coupling κ;
- the coherent generator on the private seam memory;
- the reference registers of the degree term;
- the emitter with its fuel, coupling and duration, and the timing of the reader;
- the evolution parameter of the runs with a continuous parameter (as local events the pair needs each seam to act once per round, or the limit of small event angle);
- the tangent-frame routing of the federation;
- the tree of the presence reading with its wiring and pulse schedule, and the fuel and converter that read an unrecovered seam;
- for Interval Echo, the guide, custody transfers, gate selection, relative cadence and read windows of the travelling clock, its hand, elapsed and interval widths and walk budget, the closing filter, calibrated on the reunion ratio of a reciprocal relay, and the gain and pulse of the rotation-selected port service;
- for the scalar channel, its coefficients m and c, the prepared reference with its ramps, the apparatus registers and penalties of the register form, the two operators on a profile, the pulses, the fuel dial and the bounds on a step of the observer's reference.

On 20 cells the literal allocation is 240 load registers of three states, 630 seam memories of eleven states, 180 reference registers with 180 further memories, one two-state fuel and 630 reader blocks of eleven bits. The sector of two loads on V ports has $V(V+1)/2$ states, 78 on one cell and 28,920 on 240 ports, so these tests are polynomial in the number of ports. The construction is no solver for general constraint problems and claims no polynomial bound for one [67, 68].

7 Fields, clocks and causal order

For the separate seam-field construction, write D and C for the seam-by-port gradient and face-by-seam curvature, so that $CD = 0$.

Theorem 7.1 (Local Maxwell selection)**.** *A real quadratic seam action $S(A) = \text{const} + \ell^{\mathsf{T}} A + \frac{1}{2} A^{\mathsf{T}} H A$ that is gauge invariant, has off-diagonal Hessian entries only between seams of one face, and is covariant under the sixty carrier rotations is exactly $S = \text{const} + \frac{\kappa}{2}\|CA\|^2$. For positive weights ϵ, β, a real linear autonomous evolution with $\dot{B} = -CE$, conserved $(\epsilon\|E\|^2 + \beta\|B\|^2)/2$ and reversal with E even and B odd is exactly $\dot{E} = (\beta/\epsilon) C^{\mathsf{T}} B$ on closed flux.*

Proof. Gauge invariance is $HD = 0$ and $D^{\mathsf{T}}\ell = 0$. At an edge of a face and its opposite vertex, locality permits exactly the other two edges in that entry of HD, and the signs of $CD = 0$ propagate one weight w_f over the face. Subtracting $\sum_f w_f C_f^{\mathsf{T}} C_f$ leaves a diagonal matrix annihilating D, hence zero. Transitivity on faces equalizes the weights, and the sum of the sixty signed seam actions vanishes, which removes ℓ. For evolution, conservation makes the electric block skew and fixes the cross block on closed flux, and reversal removes the skew block [7]. □

Exact rank computations and countercontrols verify the classification. The same form is the leading response of a smooth conservative field law, with a uniform finite-time bound $\|x(t) -$

$e^{tG}x_0\| \le (L/2)J_0 r^2|t|$ and no linear ansatz; exact nonlinear Gauss conservation needs an additional condition. On a supplied Euclidean domain, the complete equal-weight seam symbol Λ_a obeys $0 \le r^2 - \Lambda_a(k) \le a^2 r^4/20$ at $r = |k|$, and its reversible curl-pair group converges to the local Maxwell group with $\|U_a(t,k) - U_0(t,k)\| \le \min\{2, |t|a^2 r^3/20\}$. The premises, field identification, coefficients and clock are inputs, and native repair does not select them.

The action principle itself has a source form.

Theorem 7.2 (Derived action of a source chain)**.** *Let P be a strictly positive row-stochastic kernel on a finite state set Ω and π a strictly positive initial law. On paths with n transitions put $S_{\log}(\gamma) = -\sum_i \log P(\gamma_i, \gamma_{i+1})$ and $R(\gamma) = \pi(\gamma_0)|\Omega|^{-n}$. The Markov path law is the exponential tilt of R by $S_{\log}$ at multiplier one, with partition constant $|\Omega|^{-n}$, and a pair (S', λ') reproduces it exactly when $\lambda' S' = S_{\log} + c$ for a constant c.*

Exponentiating the negated action recovers the transition product, and row normalization telescopes the partition sum; the uniqueness clause follows by comparing logarithms at a common path, and the statements are checked in Lean [8]. The committed source chain instantiates the theorem exactly. Its bare repair count reproduces the path law at no multiplier, which makes the log-transition action the derived object. Physical field actions are a further attachment.

7.1 The native screen operator and a conditional spacetime field

On the geodesic screen of level l, let $V_l = 240 \cdot 4^l$ and prepare the uniform canonical state with total load $V_l/3$. Independent uniform seam selection and fair native repair define one complete occupation history. Write $\chi_l = q_l(V_l - q_l)/[V_l(V_l - 1)]$ for $q_l = V_l/3$.

Proposition 7.3 (Native continuum operator)**.** *Along a common refinement subsequence, the native cell Green operators converge in norm to a compact positive injective operator G on the mean-zero observation space. After restoring the constant mode, its inverse A generates a regular strongly local conservative form, with domain H^1, and*

$$n/49920 \le \lambda_n(A) \le 3n/2.$$

The complete density readouts

$$Y_l(\tau; f) = \frac{\sum_p f_l(p)[n_{\lfloor 1260\, 16^l \tau \rfloor}(p) - 1/3]}{\sqrt{V_l \chi_l}}$$

converge jointly at finite sets of times to a stationary reflection-positive Gaussian field with covariance $\langle f, e^{-|\tau - u|A} g\rangle$. The admitted coherent continuation converges strongly to $\cos(t\sqrt{A})$. With the constant mode restored,

$$\|\mathbf{1}_F e^{-\tau(A \oplus 0)} \mathbf{1}_E\| \le e^{-d(E,F)^2/(2\tau)},$$

and the cosine propagator vanishes for $|t| < \sqrt{2}\, d(E, F)$.

Proof sketch. The native cell Poincaré bound $\|(I - P_k)u\|^2 \le 624\, 4^{-k}\langle u, B_l u\rangle$ gives uniform compactness of the Green operators and norm convergence. Mosco convergence passes their local Markov forms to the limit; min–max estimates give the displayed spectrum. Conditional finite-population limits apply to the actual identity-or-swap repairs. The Gaussian heat bound gives finite propagation of the admitted cosine family [81, 82, 83, 73, 74]. □

Thus one source operator controls static covariance, relaxation and a chosen coherent wave service. Its spectral dimension is two. The $\lambda_n \asymp n$ count excludes identifying it, up to scale and bounded mass shift, with a three-dimensional elliptic bulk operator or a first-order boundary operator. A physical bulk interpretation needs an additional radial observation map. Passive repair supplies no wave sector; its attempt count and the coherent wave parameter require clock calibration. The native stationary reference supplies no physical quantum vacuum or universal area-entropy coefficient [75]. On the binary repair sector its complete instrument has unique stationary state $I_{66}/66$.

A specified radial interval and field service give the product covariance $(-\partial_r^2 + A \oplus 0)^{-1}$. If its hyperbolic coefficient density is $C = \mu\ \mathrm{diag}(-1, a)$, the effective metric is

$$g = \sqrt{-\det C}\, C^{-1} = \mu\sqrt{\det a}\ \mathrm{diag}(-1, a^{-1}).$$

The spatial coefficients are read from the source; the radial architecture, hyperbolic service and preparation are explicit design inputs.

Proposition 7.4 (Smooth effective field descriptions)**.** *Smoothing the native angular coefficients while retaining the radial Dirichlet interval gives norm-resolvent convergence, with gap $(\pi/L)^2$. For every fixed finite admissible menu of observer readouts on bounded wave times and every $\varepsilon > 0$, a smooth static $(1 + 3)$-dimensional Lorentzian metric carries a free scalar field whose complete predictions agree within ε, in addition to the stated source and clock errors.*

The proof transports the changing measures into one Hilbert space through the unitaries $U_\varepsilon f = \sqrt{\rho_\varepsilon/\rho}\, f$ and combines compact Mosco convergence with continuity of the covariance, response and finite-history operators; the complete proof is Appendix A of the spacetime paper [9]. It proves a common finite-menu approximation, without selecting a radial architecture, providing a smoothing rate, or producing a responsive metric. In this sense observers who inhabit the simulation can describe their experiences as relativistic 3+1D continuum spacetimes: the description is fixed by the predictions for their admissible readouts, and the screen is hardware of the computation, no physical space.

7.2 A causal precursor from records

The oriented conformal spherical support carries the classical isomorphisms

$$\mathrm{Conf}^+(S^2) \;\cong\; \mathrm{PSL}(2,\mathbb{C}) \;\cong\; \mathrm{SO}^+(3,1), \qquad H^3 \;\cong\; \mathrm{SO}^+(3,1)/\mathrm{SO}(3), \tag{22}$$

which identify the three-dimensional space of future unit timelike directions [53]. Authenticated records separately supply events and their order. Every quotient-visible register version carries the identifier of its last semantic writer, each commit certifies the versions its acceptance depends on, and the informational order is the transitive closure of authenticated read-from parenthood, an authenticated analogue of happened-before [43]. As an abstract finite poset it satisfies the order-theoretic causal-set axioms, and every finite causal set is the generated order of some authenticated log [1]. Twelve declared null-direction tests certify the conformal Lorentz class of a supplied invertible chart map; identifying physical events and matching their clock and cone to the field are separate source obligations [8, 9].

Theorem 7.5 (Source-derived finite (1+3) causal precursor)**.** *Let $\mathcal{L}$ be an authenticated finite semantic-event log with generated strict order $\prec_{\mathcal{L}}$ and canonical source height $h_{\mathcal{L}}$, zero on roots and one plus the maximum parent height otherwise. Then $h_{\mathcal{L}}$ strictly increases along $\prec_{\mathcal{L}}$ and equals the maximum length of an authenticated parent chain ending at each event. Let V_{src} be the rank-three source Gram quotient with positive form g_{src}, and put $W_{\mathrm{src}} = \mathbb{R} \oplus V_{\mathrm{src}}$ with $Q(t, x) = t^2 - g_{\mathrm{src}}(x, x)$.*

(F1) W_{src} *has dimension* $1+3=4$ *and* Q *has one positive and three negative directions;*

(F2) source-unit directions, S^2 *and future-null rays are exactly equivalent;*

(F3) a placement $F(e)=(\tau h_{\mathcal{L}}(e), x(e))$ *sends every generated precedence into the future cone whenever each parent edge obeys* $g_{\mathrm{src}}(x(f)-x(e), x(f)-x(e)) \le \tau^2 (h_{\mathcal{L}}(f)-h_{\mathcal{L}}(e))^2$*;*

(F4) every finite log admits an injective placement of this form that sends generated ancestry into the future cone and makes distinct same-height events spacelike; and

(F5) for a placement obeying the edge condition of (F3), if the spatial readback separates each equal-height layer and every unrelated pair with $h_{\mathcal{L}}(e) < h_{\mathcal{L}}(f)$ *is spacelike, then* $e \preceq_{\mathcal{L}} f$ *holds exactly when* $F(f)-F(e)$ *is future causal, so* F *is an exact order embedding preserving every causal interval.*

Proof. Dimension is additive and positivity of g_{src} gives the inertia; induction over parents bounds every ending chain by the height and constructs an attaining chain; the edge inequality and transitivity of cone and ancestry give (F3); an enumeration along one axis with $\tau = n+1$, n the number of events, gives (F4); and the two geometric checks exclude every unsupported cone comparison in (F5). The finite statements are formalized [1, 9]. □

Read informally, the theorem combines two things observers have. Who read whose write is a partial order, and the longest chain of reads ending at an event gives it a height. The rank-three carrier gives three spatial directions and, with a real axis, a light cone. An event placement that respects both turns the provenance order into a causal order in a four-dimensional Lorentzian carrier.

The first two clauses construct the carrier and signature from an independent real axis and the rank-three source carrier, without assuming a rank-four chart; source height enters only through placements, and the scaled height is no operational clock. A physical manifold requires a source-causal continuum certificate: one refinement family supplying physical event identification, source-selected order and cone embeddings, refinement maps, a calibrated count density, agreement across independent dimension and manifoldlikeness tests against Poisson-sprinkled controls, and convergence to a distinguishing time-oriented Lorentzian geometry [34, 35, 36].

Proposition 7.6 (Composition of the continuum certificate)**.** *For a source-causal continuum certificate, causal order fixes the conformal Lorentzian geometry of the admitted distinguishing limit and the calibrated count measure fixes its conformal scale [41, 42]; the local model is* $(1+3)$*, so a limit satisfying the dimension and topology clauses of the certificate is an effective four-dimensional time-oriented Lorentzian event manifold. If on the same family a causal-set d'Alembertian or scalar-curvature estimator converges as an independent curvature diagnostic [39, 40], an explicit tensor-curvature reconstruction converges to the Einstein tensor or the small-ball null-balance route identifies the limiting geometry tensor with* G_{ab}*, and stress and Ward–Bianchi data converge with calibrated coupling, then the smooth limit is* $G_{ab}+\Lambda g_{ab} = 8\pi G\, T_{ab}$*.*

A source-record population realizes the flat case.

Theorem 7.7 (A source-record causal and count limit)**.** *In the rank-three conservative repair carrier, let* $\varphi = (1+\sqrt{5})/2$*,* $L = 2/\sqrt{\varphi+2}$ *and* $q = F_n$ *the* n*-th Fibonacci number,* $n \ge 4$*. The population* $S_q = L\{b\varphi - \lfloor b\varphi \rfloor : 0 \le b < q\}^3 \subset [0,L]^3$ *consists of* q^3 *distinct conservative source-record images. Retain it at each layer and let every next-layer event read all preceding-layer sites within* $a_q = L/\sqrt{q}$*, with model duration* $\Delta_q = a_q/c$ *for a declared speed* c*. As* $q \to \infty$ *the order*

converges away from null separation to the speed-c causal order, and with $\rho_q = q^3/(L^3\Delta_q)$, for fixed interior timelike diamonds,

$$\frac{|I_q|}{\rho_q} \longrightarrow \mathrm{Vol}(I), \qquad \frac{2C_q}{|I_q|(|I_q|-1)} \longrightarrow \frac{1}{10},$$

where C_q counts strict causally ordered pairs; for vertical duration T, $\mathrm{Vol}(I) = \pi c^3 T^4/24$.

Corollary 7.8 (Proper-time ratios from record counts)**.** *If I_q, J_q approach interior timelike diamonds of proper durations $\tau_I, \tau_J > 0$, the observer readout $R_q(I;J) = (|I_q|/|J_q|)^{1/4} \to \tau_I/\tau_J$. Within positive volume-only readouts additive on collinear inertial intervals, the fourth root is unique up to units.*

At finite regulator the population is produced by the carriers themselves: each holds its record as port loads, reads its position through the rank-three response and decides its neighbors from that readback, and the precedence generated from their authenticated reads equals the layered order through $q = 89$, that is 704,969 carriers reading one another over ten rounds. On the largest interior diamond the inverted Myrheim–Meyer dimension reads 2.83, 4.38, 3.55, 3.84 and 3.92 at $q = 13, 21, 34, 55, 89$ [37, 38]; the readings at $q = 5$ and $q = 8$ lie below the regime of the theorem. The ordering fraction of the central diamond reads 0.088, 0.138, 0.092, 0.093 and 0.094 against the proved flat value 1/10, and the count clock reads 1.71, 2.09, 1.91 and 2.05 at $q = 13, 34, 55, 89$ against the model-time ratio 2. Covariance requirements select the cone: a closed convex pointed displacement cone preserved by the irreducible icosahedral rotations and by boosts along one axis is the future or past cone of $t^2 - \|x\|^2$. The read law and model clock are declared, and the ordinal height of a history with self-waits is no proper-time instrument [9].

The native seam event has its own finite causal bound. For a fixed seam schedule and shared local coins, dependence crosses at most one seam per ordered repair event, and retained signal witnesses attain the bound; this is a speed in seams per native event. Remote repairs can carry a difference to a receiver before its first local tick, so the bound is not one seam per receiver tick [76]. Complete endpoint records give a forward-cone placement in the registered response geometry, and a four-event native execution has a Lean instance proving that implication and the failure of its converse [1]. In the executable model the records depend on the local order of events alone (Section 6.4), and the travelling clocks of Interval Echo compare durations at reunion (Section 6.5).

8 Gauge structure, centre classes and bound objects

The finite theorem fixes a current algebra under explicit response premises. A chosen carrier and memory law then realize its currents. These are different steps of one construction: the Lie type constrains admissible interactions, while the executable specification fixes what its port services generate. Recovering or choosing that specification is allowed; its agreement with physical particle records is an additional requirement.

8.1 The finite gauge theorem and matter representation

Let A be the icosahedral adjacency matrix and J its antipodal involution. Exact incidence gives

$$10J = A^3 - 4A^2 - 5A + 10I, \qquad P_{12} = \mathbf{1} \oplus \mathbf{5} \oplus \mathbf{3} \oplus \mathbf{3}'. \tag{23}$$

The even port coordinates carry $\mathbf{1} \oplus \mathbf{5}$; the odd coordinates carry the two triplets. The response premise of Section 2.2 requires an injective derivative $D : P_{12} \to \mathfrak{u}(H)$, a commutator-closed image

with positive trace pairing, and internal implementation of every proper carrier rotation. Internal implementation means that its projective implementer factors into the connected response group and a pointwise centralizer. This is the response-endogeneity clause identified as A2 in the library; it is not implied by the port count alone [84, 11].

Theorem 8.1 (Gauge Lie-type forcing)**.**
Under these complete-response and internal-implementation premises,

$$\mathfrak{g} = D(P_{12}) \cong \mathfrak{u}(1) \oplus \mathfrak{su}(2) \oplus \mathfrak{su}(3).$$

Its center is the uniform port line. The three-dimensional simple ideal carries one triplet, and the eight-dimensional ideal carries the other triplet and the five-dimensional band.

Proof. The trace pairing makes the twelve-dimensional image compact. Internal implementation makes the A_5 action inner, so it fixes the center pointwise. The transitive port action has a one-dimensional fixed space, hence the center has dimension at most one. With zero center, the only compact semisimple type of dimension twelve is $\mathfrak{su}(2)^4$. Inner automorphisms preserve its simple ideals, each of which has either zero or three A_5-fixed directions, contradicting the one-dimensional fixed space. The center therefore has dimension one; the unique compact semisimple type of dimension eleven is $\mathfrak{su}(2) \oplus \mathfrak{su}(3)$ [64]. □

The premises have an explicit finite matrix realization. Six antipodal axis vectors form a matrix U over $\mathbb{Q}(\sqrt{5})$; $\sigma(U)$ is its Galois conjugate. For even coordinates b, odd coordinates d, and $c = \frac{1}{6}\sum_i b_i$, put $\Phi_0(b - c\mathbf{1}) = \sum_i (b_i - c) u_i u_i^{\mathsf{T}}$. For nonzero real band coefficients,

$$K(f) = \operatorname{diag}\Big(\lambda_3 \widehat{Ud} + i[\lambda_1 c I_3 + \lambda_5 \Phi_0(b - c\mathbf{1})], \lambda_{3'} \widehat{\sigma(U)d}\Big), \qquad \widehat{x}y = x \times y. \tag{24}$$

Proposition 8.2 (Finite response realization)**.** *The map K is injective and equivariant, its image is commutator-closed, and proper carrier rotations act internally. Its pulled-back bracket has*

$$(P_{12}, [\ ,\ ]_K) \cong \mathfrak{u}(3) \oplus \mathfrak{so}(3). \tag{25}$$

The six axis projectors span the symmetric matrices, while the triplets span the skew matrices in the two blocks. These rank and equivariance identities are exact over the full sixty-element rotation group. The representation and nonzero coefficients are design inputs. A zero bracket on the same port module violates the internal-implementation premise; it is not excluded by geometry alone. The gauge specialist gives the complete finite certificate and the boundary between analytic classification and machine-checked algebra [11].

Theorem 8.3 (Finite matter image)**.** *For the supplied trace-balanced module $V = \mathbb{C}^3_{-1/3} \oplus \mathbb{C}^2_{1/2}$,*

$$\Lambda^2 V \oplus \Lambda^4 V = Q \oplus u^c \oplus e^c \oplus d^c \oplus L, \tag{26}$$

where $Q = (3,2)_{1/6}$, $u^c = (\bar{3},1)_{-2/3}$, $e^c = (1,1)_1$, $d^c = (\bar{3},1)_{1/3}$ and $L = (1,2)_{-1/2}$. All perturbative gauge and mixed gravitational anomalies vanish, the number of weak doublets is even, and the faithful image is

$$\frac{\mathrm{SU}(3) \times \mathrm{SU}(2) \times \mathrm{U}(1)}{\mathbb{Z}_6}. \tag{27}$$

Among the 1,024 *subsets of the ten nontrivial irreducible exterior summands, nonemptiness, chirality and the four anomaly-trace conditions select exactly this fifteen-state mask and its charge conjugate.*

The exterior branching, anomaly traces and center kernel are finite calculations [11]. The supplied module is the familiar $\mathbf{10} \oplus \overline{\mathbf{5}}$ branching; this result does not require a physical SU(5) gauge field. It does not fix the number of families.

The record law of committed repair realizes this global form. It is covariant under independent phases on the twelve ports; read on the protected code, twelve relative port phases per seam generate exactly $\mathrm{S}(\mathrm{U}(3) \times \mathrm{U}(2))$, the group (27). Its centre is the circle $\{\mathrm{diag}(e^{2it} I_3, e^{-3it} I_2)\}$; the $\mathbb{Z}_6$ of (27) is the kernel of the covering product, and the order-six central subgroup generated by $e^{2\pi i Y}$ is the flux alphabet of the protected defects (Section 8.3). The native transports alone form a finite group, and the continuous port phases are a declared extension [11].

8.2 The port response of the executable model

Theorem 8.1 consumes twelve port generators that are independent, closed under commutators and carry a positive trace form, with the rotations of the cell acting through them. The contrast-memory law on one cell is tested against this premise. A port service is a weak operation by the observer of one port that lasts long against the inverse level spacings of the law, so that it acts through its part diagonal in the levels. The response space is the pair of triplets $\mathbf{3} \oplus \mathbf{3}'$ of (2): for one load the slow and the fast level of Section 3.4, for the bound pair its two lowest triplets that are odd under the antipodal map. The matrices of this subsection are audit, and no observer reads them.

The plain services of the law are the load of each port, the exchange of each seam and the twist of each port, its circulation round the five neighbours. The loads generate seventeen dimensions, two copies of $\mathfrak{su}(3)$ and one common number, for one load and for the bound pair at $\kappa = 8$. So do the exchanges of the seams, and so does load and twist taken as one service per port; all plain services together generate eighteen. The count follows from a lock between the two triplets: every operator at a port with rational entries acts on the fast triplet as the conjugate under $\sqrt{5} \mapsto -\sqrt{5}$ of its action on the slow triplet, so the closure holds $\mathfrak{su}(3)$ twice.

One declared service gives twelve. Let $H_1 = L/2$ be the law of one load without its constant, $E_{\mathrm{top}} = (5 + \sqrt{5})/2$ its top level and J_v the twist of port v, and put

$$F_v = \tfrac{1}{2}\{n_v,\, E_{\mathrm{top}} - H_1\} + J_v. \tag{28}$$

The twelve F_v are independent and close under commutators into $\mathfrak{u}(3)$ on the slow triplet and $\mathfrak{so}(3)$ on the fast one, the form (25). Their trace form is positive, with eigenvalues between 0.5 and 7.24. The 66 brackets lie inside the span with residual 9×10^{-15}, the 720 covariance identities of the 60 rotations hold with residual 2×10^{-15}, and the generators of the rotations lie inside the span. The weighting, whose coefficient is tied to a level of the law, and the twist are supplied; the law's own events provide neither. On the bound pair the same construction gives twelve when the load is weighted from the pair's own $\mathbf{3}'$ level, which uses knowledge of the target level, and seventeen when it is weighted from the top of the bound levels. No service of the law's own events that gives twelve on the composite is exhibited.

Interval Echo selects its port service from the rotations of the cell. The twelve rotations by a fifth of a turn sum to a class operator, and its positive spectral projector P selects the response; the service of port p is the band-diagonal part of $Pn_pP + J_p$ with unit gain. On one load and on the bound pair at $\kappa = 8$ the twelve services are independent, all 66 brackets lie in their span, and the 720 rotation-conjugation checks hold with residual norms below 10^{-11}. Prepared overlap transport generates all 60 proper rechartings on 20 and 80 cells with a matching unit-gain implementer. A signed pulse of the current at one port changes the distribution of the bound pair's seam readings by up to 0.11 in total variation, so the observers of the cell read these currents. Admitting the bare

load of a port as a further service enlarges the visible closure to 17 directions, and the completeness of the physically accessible menu is the premise on which the inference to the gauge algebra rests [68].

Two exact couplings appear in this audit. Count energies from 12κ, the energy of two free loads in the uniform mode. At $\kappa = 1$ the triplet levels of the pair are $2 - \sqrt{5}$, $(7 - \sqrt{5})/2$, $2 + \sqrt{5}$ and $(7 + \sqrt{5})/2$, and on the second and the fourth the load of every port is exactly $1/6$ with vanishing twist. At $\kappa = (\sqrt{5} - 1)/2$ a pair on a seam costs exactly what two free loads in the slow level cost, $5 - \sqrt{5}$. No selection of the coupling is claimed.

8.3 Protected centre classes

A protected defect on a carrier face holds a flux class $k \in \mathbb{Z}_6 = \mathbb{Z}_3 \times \mathbb{Z}_2$, a colour-centre charge with a weak-centre parity, and the classes on one closed carrier add to zero. A quantum's internal pattern is an occupation (n_3, n_2) of the five-level code $V = \mathbb{C}^3_{-1/3} \oplus \mathbb{C}^2_{1/2}$, with $6Y = 3n_2 - 2n_3$.

Theorem 8.4 (Native flux and centre-character dictionary)**.** *The kernel element* $(\omega I_3, -I_2, e^{2\pi i Y})$ *of the covering product acts as the identity on all* 32 *patterns, and a flux of class* f *acts on a pattern by the phase* $e^{2\pi i f \cdot 6Y/6}$*. The class seen by a pattern is*

$$k \equiv 6Y \pmod 6, \qquad k \bmod 3 = n_3 \bmod 3, \qquad k \bmod 2 = n_2 \bmod 2,$$

and the class multiplicities are $(4, 6, 6, 4, 6, 6)$*.*

Proof. ωI_3, $-I_2$ and $e^{2\pi i Y}$ act by ω^{n_3}, $(-1)^{n_2}$ and $(-1)^{n_2}\omega^{-n_3}$; the rest is reduction of $6Y$ modulo 3 and 2. □

Table 9: Native flux classes and compatible Standard Model centre characters. A class does not uniquely identify a physical species.

k	Centre characters	Particles
$1, 5$	$\omega^{\pm 1}$, -1	left-handed quarks Q and antiquarks
$4, 2$	$\omega^{\pm 1}$, $+1$	right-handed quarks and antiquarks
3	1, -1	lepton doublet and Higgs doublet
0	1, $+1$	e_R, ν_R, photon, gluons, W, Z

A quantum of class k taken around a flux of class f gains the phase $e^{2\pi i f k/6}$, so colour flux is seen only by quarks and weak flux only by the weak doublets, the left-handed fermions and the Higgs. The central involution z of the carrier's rotation cover acts on the code as $\mathrm{diag}(1, 1, 1, -1, -1) = e^{i\pi \cdot 6Y}$.

The class is the centre class. It carries neither the generation nor T_3, so up and down, electron and neutrino, and colour singlet and octet share a class. The executable certificates check every pattern in exact arithmetic [12, 1].

The same code fixes the couplings of the links at the cell. The seam cost of a code state carried around a plaquette, averaged over the code, is $1 - \mathrm{Re}\,\mathrm{tr}_5\, U_P/5$, and this trace gives equal bare couplings $g_3 = g_2 = g_1$ in the grand-unified normalization at the cell, so $\sin^2\theta_W = 3/8$ there, and gluons, W and B travel on one cone. Restricted to a colour holonomy W the cost is $(3/5)(1 - \mathrm{Re}\,\mathrm{tr}\, W/3)$, the Wilson plaquette action with $\beta = 6/g^2$, and the colour centre is the pair of flux classes 2 and 4. A Monte Carlo study of these links at $N_t = 4$ finds a first-order deconfinement transition at $\beta_c = 5.69105(39)$, where the published value for this lattice theory is 5.6925(2) [11, 26]. The equality holds for the bare couplings of this action, and the study holds the links alone at one lattice spacing.

8.4 Bound objects of the contrast-memory law

Under the law (11) an object is a set of loads. A load counts 6 in C and every agreed seam takes 2 off, so an object of N loads with m agreed seams costs $6N - 2m$. Table 10 lists the cheapest objects on one cell. The first three are a port, a seam and a face, the three kinds of centre of the cell: 12 ports, 30 seams and 20 faces, 62 axis points in all. Every object gains at least 2 against every split into two parts.

Table 10: The cheapest objects of N loads on one cell under the contrast-memory law. The cost is the value of C; the last column is the least gain in C against a split into two objects.

N	**Shape**	**Number**	**Agreed seams**	**Cost**	**Gain**
1	one port	12	0	6	
2	one seam	30	1	10	2
3	one face	20	3	12	4
4	two faces on a seam	30	5	14	4
5	three faces round a port	60	7	16	4
6	a port and its five neighbours	12	10	16	6
12	the whole cell	1	30	12	10

At finite coupling the lowest level of N loads on one cell lies below N free loads by the binding B_N of Table 11, in units of the exchange. These levels are audit on the spectrum. In the lowest level of two loads the pair is on a seam with probability 0.60, 0.86, 0.99 and 1.00 at $\kappa = 0.5$, 2, 8 and 128. Inside a cell the exchange takes a pair from one seam to the seams of the adjoining faces at first order. From the seams of one cell to those of the next the transfer passes through one separated state and has amplitude $1/(8\kappa)$.

Table 11: Binding B_N of the lowest level of N loads on one cell against N free loads, in units of the exchange.

κ	B_2	B_3	B_4	B_5	B_6
0.5	0.526	1.556	3.049	4.965	7.277
1	1.185	3.546	6.864	10.905	15.816
2	2.779	8.554	15.927	24.206	35.305
8	14.236	43.728	75.212	107.678	155.076
128	254.016	763.513	1275.013	1787.511	2555.005

These objects are read on ports, seams and faces by the observers of their cells. What they need for a physical reading is listed in Section 11.

The electron's charge and field response. A written-field extension of Interval Echo provides a candidate for this part of the electron. One load more or less than the filled reference changes the signed boundary flux by a whole unit in individual transfer records. With source material held in its launch cell, a material probe responds 22 cell steps away on a prepared 320-cell federation. A magnetic twist changes the load's return probability. These results establish a mobile signed charge coupled to the written field of a modified seam law [68].

On the registered blank seams, a vacancy and an excess each transport two coherent orbital modes through two cell boundaries. A controlled full turn preserves their phase. Exchanging two encoded defects carries their reference associations across the two owners with positive exchange phase. An unsteered two-defect flight distinguishes the native scattering law from a sign-reversed

exchange law. The first amplitude to reach a neighbouring cell from any localized launch has one quarter of its weight in the triplet of the registered one-load colour meter. Applying the corresponding singlet filter to a signed defect at both ends permits coherent orbital transfer. These readings distinguish an endpoint colour outcome from colour neutrality throughout propagation [68, 12].

Four joined faces supply two field states that change how that load moves. Both can cross a gateway with the charge. An addressed exchange of two material loads restores the complete field word and leaves the orbital labels at their original gateways. At most 1.1072% of any prepared doublet lies in the lowest charged level of this finite guide, and its energy has no independent conversion to keV. The physical spin, statistics and mass of an electron must be measured for the same mobile excitation [12].

9 The Einstein equation from a realized null balance

The gravitational hypothesis identifies Einstein dynamics with the coarse response of the same process.

Theorem 9.1 (Null tomography and metric ambiguity)**.** *Let V be four-dimensional with Lorentz form η of signature $(-,+,+,+)$, the opposite convention from Q in Section 7.2; nothing below depends on the choice. If a symmetric form X satisfies $X(k,k)=0$ for every null vector k, then $X=\phi\eta$. Null-null values therefore determine a symmetric tensor modulo the metric line, and nine explicit null directions, the six axis rays $(1,\pm e_i)$ and $(1,s,s,\pm s)$, $(1,s,-s,s)$ with $s=\sqrt{3}/3$, reconstruct the quotient $\mathrm{Sym}^2(V^*)/\mathbb{R}\eta$ with design determinant $8192/27$ in the certificate's basis and a decoder obeying $\|x\|_\infty \le (2+\sqrt{3})\|q\|_\infty$.*

Proof. On future null rays $(1,n)$ the identity $X_{00}+2X_{0i}n_i+X_{ij}n_in_j=0$ on the unit sphere forces $X_{0i}=0$, $X_{ij}=\phi\delta_{ij}$ and $X_{00}=-\phi$. The determinant and decoder bound are exact calculations, and the design, injectivity and ambiguity are formalized in Lean [1, 9]. □

The same decoder gives the sharp entrywise error bound $(2+\sqrt{3})\epsilon$ for null-charge errors at most ϵ. A Ward residual w bounds the remaining metric coefficient by $|c(x+e_j)-c(x)|\le aw+8(2+\sqrt{3})\epsilon$ for forward differences. Centered derivatives control only two-step differences; the exact checkerboard counterexample forbids substituting nearest-neighbour connectivity. These finite error inequalities are machine-checked [1].

Theorem 9.2 (Tensor completion of a realized null balance)**.** *Let (M,g) be a connected, time-oriented, C^3 Lorentzian four-manifold and T_{ab} a symmetric C^1 tensor with $\nabla^a T_{ab}=0$. Suppose a common realized tower supplies the gravitational normalization $8\pi G_N>0$ with*

$$G^{(g)}_{ab}k^ak^b = 8\pi G_N T_{ab}k^ak^b \tag{29}$$

for every null vector k at every point. Then there is a constant Λ with

$$G^{(g)}_{ab}+\Lambda g_{ab} = 8\pi G_N T_{ab}, \tag{30}$$

and a reference event at which the difference equals $-\Lambda_0 g_{ab}$ fixes $\Lambda=\Lambda_0$.

Proof. Theorem 9.1 applied pointwise to $G^{(g)}-8\pi G_N T$ gives $G^{(g)}_{ab}-8\pi G_N T_{ab}=\phi g_{ab}$. The contracted Bianchi identity, the Ward premise and metric compatibility give $\nabla_b\phi=0$, connectedness makes ϕ constant, and $\Lambda=-\phi$. □

Null balance fixes Einstein's equation up to a metric term; the Bianchi identity and stress conservation make its coefficient the cosmological constant. The coefficients of entanglement-equilibrium arguments [60] enter through one machine-checked identity: scalars with $\delta S_{\mathrm{bulk}} = \frac{8\pi^2\ell^4}{15}t$, $\delta A = -\frac{4\pi\ell^4}{15}f$ and $\delta S_{\mathrm{bulk}} + \delta A/(4G_N) = 0$ obey $f = 8\pi G_N t$. For OPH to supply (29), one common refinement tower must realize (G1) the effective manifold of Proposition 7.6; (G2) geometrically normalized cap modular flow whose directional charges define one stress tensor; (G3) its Ward identity, independently of that reconstruction; (G4) the edge-center entropy split, the normalization $\delta\langle Z_L\rangle = \delta A/(4G_N)$, the modular first law and generalized-entropy stationarity; (G5) a small-ball family with controlled remainders and enough observer directions; and (G6) universal coupling, a vacuum reference and a scale calibration fixing $8\pi G_N$. The finite layer contains null tomography, the edge-entropy split and the coefficient identity, and the machine-checked composition proves the tensor step from an explicit null-balance premise; the bridge between them is (M4).

Interval Echo supplies a finite energy-continuity identity on the 20-cell sphere. Assigning half of each intercell bond energy to each incident cell makes regional energy additive. For two neighboring cells and their union, the energy derivative equals the oriented sum of boundary currents as an operator on all 28,680 configurations with two distinct occupied ports. Local bond probes reproduced the energy derivatives to within 2.7×10^{-8} in twelve comparisons. In a prepared regional reference, a sequence of coherent filters applies weights from the three-component slow response to the native seam energies. The resulting modular charge predicts six independently computed variations of this weighted matter energy to within 10^{-5} in exchange units. The same parent repair Hamiltonian predicts the modular energy after restriction to nested and overlapping patches. On a held six-port patch the independent measurement gives 0.686 units and the prediction gives 0.685. Retaining only the interior seams gives 0.125. On one rotation-averaged reference, the modular readings of twelve overlapping stars restrict to a quadratic in direction on the constant mode and the first spatial triplet. Nine prespecified readings predict the other three within 2.60 propagated standard errors on two preparations at two exposures. A sharp load misses by 5.99 nats. The reference symmetry is supplied. The tensor interpretation requires geometrically normalized stress and independent curvature [9].

A second native experiment calibrates an ordinary source with a vacancy probe. The calibration predicts the response of an excess probe on other bridges. Yet a completely mixed probe develops polarization, which every unitary on the measured two-port space would leave zero. In free flight with all ports available, a uniformly mixed probe also resolves correlations between two seams close to its receiver. Moving the same energy increment into stationary seam memories breaks the ordinary-source calibration. These measurements resolve a material interaction. Testing universal gravity requires independent curvature and directional stress on those preparations.

In a homogeneous Bianchi I comparison, two quantized scalar fields source a classical metric through a specified Einstein Hamiltonian. Calibration on the first field predicts the second field's gravitational coupling. At the finest radar resolution its inferred ratio to the first lies between 0.99986 and 1.00011 on nine held comparisons. Halving the second coupling in the Hamiltonian gives ratios near 0.5 by radar and by the independent shrinking-ball area measurement. With a bilinear matter interaction, two entangled preparations have identical individual field states and opposite joint correlations. The measured cross covariance and independently measured frequency splitting predict a change of 0.0029654 in G_{00} in box units. Radar gives 0.0029684 and the area at fixed proper volume gives 0.0029695. Removing the interaction removes the geometry difference. The experiment measures semiclassical sourcing under the declared dynamics. Transferring this result to Interval Echo requires a native curvature measurement [9].

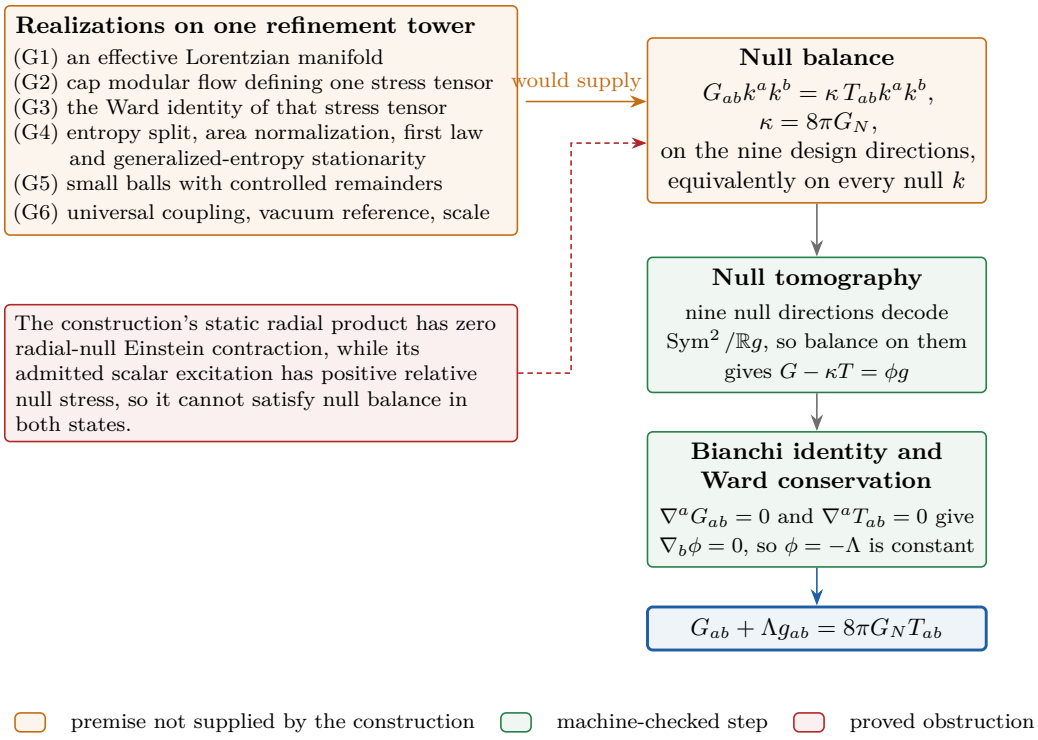


Figure 8: The Einstein equation as tensor completion of a realized null balance (Theorem 9.2). The tensor step is machine-checked from an explicit null-balance premise. Realizations (G1) to (G6) on one refinement tower would supply that premise, and no complete realization of them on one common refinement tower is established; the tested static radial product fails the balance for its own scalar excitation.

10 Cosmology and the closure coordinates

The cosmological hypothesis asks the same process to fix the vacuum, the dark sector and the primordial response. In this paper the layer consists of conditional branches and diagnostics of declared maps.

10.1 The dark sector: non-luminous charge, the deep galaxy law, and the vacuum coordinate

Under supplied universal-coupling, physical-stress and source-localization premises, sourcing gravity by modular charge classifies any geometric excess over the luminous term as non-luminous modular charge, with anomalous modular energy on overlap collars as one candidate carrier [14]. Conditional on two named premises the deep-regime profile is characterized rather than supplied: an enclosed-mass law that is degree-one scale covariant and composes independent sources in quadrature carries a unique constant $a_0 > 0$ with $M_A(r) = r\sqrt{M_b a_0/G}$, which forces flat rotation curves and gives $v^4 = GM_b a_0$, the baryonic Tully–Fisher relation, each premise load-bearing by an explicit counterexample. A per-cut model gives $a_0 = Gn^2c$, with only the product n^2c identifiable, and the value of a_0 requires an independent source measurement. A scale calibrated on 74 galaxies misses one of 151 exterior rotation speeds by at least 5.49 quoted errors with the catalogue geometry and extended baryonic force. Independent stellar distances and inner-disk inclinations admit a simulta-

neous fit when the nuisance parameters are selected on those speeds [14]. Reading the dark-energy density as $\rho_{\rm DE} = \kappa/N$ at constant κ, with the separately conserved Friedmann continuity law, gives $w = -1 + \frac{1}{3}\,\mathrm{d}\ln N/\mathrm{d}\ln a$, so fixed capacity gives the exact point $(w_0, w_a) = (-1, 0)$ and nondecreasing capacity gives $w \geq -1$; exclusion of that point fails the fixed branch, while agreement supports nothing, since it is also the ΛCDM null [15].

A finite patch can distinguish a modular-charge fluctuation from a change in stored energy. At fixed energy histogram, a material interferometer reads signed collar charges near ± 0.091 nats. Reversing a retained preparation bit preserves the fluctuation amplitude, while mixing the two tagged preparations equally makes it vanish. Linearity excludes a fixed single-preparation mean for all three amplitudes. Two distinct writes conditioned on the same bit measure the variance through their centred product. A travelling probe detects the shared history even with the bit hidden and ordinary occupancy fixed. In an independent instrument, adding ordinary occupancy changes the initial relative angular acceleration of two tracers. The variance intervention leaves that acceleration exactly unchanged because it preserves all four mean contact energies. Converting the measured fluctuation to gravitating stress requires a physical modular reference and a metric response calibrated on ordinary matter [14]. For the spherical deep profile with negligible slip, differences of orbital mass and projected shear across a common annulus obey a parameter-free equality even with unknown compact inner mass [14].

10.2 Expansion, horizons and records

Expansion adds no causal data to the layered read law. A physical read $\|\sigma_{j+1}t - \sigma_{j+1}s\| \leq \sigma_{j+1}a$ holds exactly when $\|t - s\| \leq a$, so every scale-factor profile generates one order, as conformal invariance of causal structure requires [41, 42]. The profile enters only the count measure: a constant physical event density gives the four-volume weight $\sigma^4\, d\eta\, d^3x$, and the source law does not select σ [16]. On a finite screen of fixed capacity, maximizing generalized entropy over sector probabilities gives $S_{\rm gen}^{\max} = \log M$, and uniform transfer of a fraction f of the horizon capacity to an observer changes that maximum by $\log(1 - f) < 0$, the sign of the de Sitter time advance [13]. Public records keep an exact information ledger: pinching is an average of independent sign unitaries whose entropy gain equals the relative entropy to the pinched state, and on a supplied three-dimensional layered population crossing reads obey an area law with coefficient $(\pi/4)n^2a^4$. A declared nat per crossing calibrates that area; horizon entropy, Hawking flux and evaporation need the native channel and a physical geometry [17].

10.3 Pixel closure and the record capacity

The dimensionless pixel coordinate is $P = a_{\rm cell}/\ell_P^2$. Its self-reference equation relates it to a response computed from the chosen source specification,

$$P = \varphi + \frac{\sqrt{\pi}}{A(P)}, \qquad \varphi = \frac{1 + \sqrt{5}}{2},$$

where A is the declared inverse electromagnetic-coupling readout. A fixed-point proof determines a root of that map. Identifying its readout with the physical Thomson coupling requires the current response of the same action, vacuum, spectrum and clock.

The specialist coupling analysis evaluates the readout with supplied running slopes, thresholds and scale forms [10]. Agreement obtained by selecting those inputs does not derive the current response of an interacting source. A complete physical loop must replace the coefficient readout by the current spectral response of the actual interacting states, and closing the displayed scalar map

does not close that loop. Detector use of $g(P) = \sqrt{4\pi\alpha(P)}$ reads a supplied coupling; it does not independently derive its electromagnetic meaning.

A separate exact scalar is due to Wissner-Gross [18]. For four slots of dimensions $(3, 2, 3, 2)$, traceless letters on unordered slot pairs give 169 product records and three exchange-odd directions complete a 172-dimensional feature space. Two commuting signed exchanges X, Y define $K = (2I - X)(3I - Y)/2$, whose joint projectors have gains $1, 2, 3, 6$ and ranks $79, 48, 42, 3$. With the declared normalization 31104,

$$\alpha_{\text{pair}} = \frac{79 + 48\sqrt{2} + 42\sqrt{3} + 3\sqrt{6}}{31104}, \qquad \alpha_{\text{pair}}^{-1} = 137.035999189566\ldots,$$

against the measured 137.035999177(21) [19]. An independent reconstruction verifies the arithmetic with no continuous coefficient. Its identification with the Thomson coupling, its normalized-trace readout and its attachment to the screen grain are conditional [10].

The other closure coordinate, record capacity N, bounds the declared correctable record algebra. Under its de Sitter entropy interpretation,

$$N = \frac{3\pi}{\Lambda \ell_P^2}, \qquad \ell_P^2 = \frac{\hbar G}{c^3}. \tag{31}$$

This dictionary converts a capacity into a cosmological constant after physical scale calibration. It does not make a fitted capacity an independent cosmological prediction. The specialist analyses separate conditional root certificates, measured-coordinate comparisons and independent physical tests [10, 15].

11 Realized results and physical obligations

The physical target is one realization whose limiting observable laws agree with measurement. Finite certificates establish their displayed domains; calibration and physical identification are separate statements. Table 12 collects the constructed results, their requirements and the negative controls that delimit them, for the theory and for the candidates of the executable model. The criterion for refinement and for physical extension is agreement of the distributions of admissible observer records with what observers in our world record. Observers who inhabit the simulation can describe their experiences as relativistic 3+1D continuum spacetimes: that is the content of Proposition 7.4 with the rank-three spatial carrier and the causal and count limits, under their stated premises. The obligation of the model is to supply those premises with its own local clocks and records; it does not have to rebuild three dimensions inside its state. The outputs that meet premises of finite theorems as they stand are the carrier with its rank-three band, the seam rule, complete instruments with projective readings, record algebras with certain rereads, count clocks compared through shared records, travelling clocks whose reunions follow the proper-time forecast, the twelve-dimensional response under one declared service and the rotation-selected currents of Interval Echo, and the information projection of two overlapping observers (Table 8). A difference between microscopic state encodings is no failure of the model, and a resemblance between them is no success. Existence and phenomenal experience are interpretive questions: an implemented record interface does not derive why anything exists or the phenomenal character of a record. The executable-model paper lists the supplied parts and the limits of the construction [67].

Table 12: Constructed domains and their physical extension. The stated failures apply to their tested member or identification. For the candidates of the executable model the second column states what they realize and the third what their physical reading needs.

Domain	**Constructed result**	**Required extension and negative controls**
Observers and records	Finite consensus normal forms, complete instruments, quantum identities and repair entropy laws	The declared preparations, algebra, scheduler and resource accounting must belong to the same process. Classical committed records alone supply no Bell violation; consensus does not select a unique physical history.
Space and fields	Exact rank-three carrier response, causal event records, controlled field limits and smooth effective field descriptions	Physical position and common clocks require realization. Full-port refinement loses the rank-three band and the screen has spectral dimension two; these are properties of the hardware of the computation and no test of the effective description.
Gauge and matter	Conditional Standard Model Lie type, a declared matter representation and centre characters	Centre classes do not identify species. Charges, spin, statistics and mixing must be recovered on one process and one compatible physical limit.
Gravity	Null tomography and tensor completion with exact decoder constants	The metric, conserved stress, generalized entropy and clocks must realize one refinement tower. The tested static scalar member fails its null balance.
Cosmology	The capacity equation of state, the deep-law implication, the closure coordinates and public-data comparisons	Vacuum, horizon and physical-scale selection are explicit. Shared-data alternatives are not independent confirmations.
Interval Echo and its contrast-memory seam		
Travelling clock	A patch carries its hand, elapsed count and interval memory through verified handoffs; at reunion the ratio of the two counts follows the proper-time forecast from the observers' own light-pulse speeds within about one part in a thousand, and a wider clock extends the range (Section 6.5)	Held clock constructions and directions, and transport of the three directions by the full records of a moving observer.
Overlapping observers	Single-cell and overlapping three-cell observers of the 320-cell sphere agree on every shared checkpoint; a local priority joins a repair fork; two overlapping observers realize the unique information projection	An authenticated causal order with count and volume limits, and confluence of every accepted repair on the federation.
Port currents	Twelve rotation-selected currents, independent and closed under commutators on one load and on the bound pair, with all sixty rechartings by overlap transport (Section 8.2)	Completeness of the physically accessible menu, and one common measurement of current and stress on a bound excitation.

Table 12 continued

Domain	Constructed result	Required extension and negative controls
Memory realization	The echo on the private seam memory is given on all 99 local states and reduces exactly to the law on loads on blank memory, for every coupling (Proposition 3.4)	A selection of the coupling κ, which is supplied.
Binding	A pair on a seam is bound at every reading on every federation of complete cells (Theorem 6.1); the exchange law alone loses it	An identified antiparticle and annihilation channel, and the class of an object as a record.
Bound objects read on other seams	The pair and the face object are read on other seams and faces; the cheapest objects of one cell are listed in Table 10	One limiting speed for all objects: the bound pair is a Galilean composite, with branch $E(K) = \Delta - \cos^2(K/2)/\Delta$, $\Delta = 1 + 2\kappa$, on a chain, and free clusters of two, three and four loads have kinetic ratios that differ from their rest-energy ratios. A refinement map that preserves seams; the test of a refinement is agreement of the distributions of admissible observer records between levels.
Agreed records	A complete instrument of seam records from the two ends of every seam, with the outcome "no pair"	A record of currents that later events read, and a seam connection with its own energy.
Events with no common clock	Records depend on the local order of events alone; rounds keep the pair with unequal counts	Normalization of every clock of the model to proper time, which the travelling clock meets on the tested journeys.
The unrecovered collar	The recovery state of every seam is conserved; an unrecovered collar holds no load and lies one agreement energy above the recovered seam; a load on one of its ports binds to it; its observers read its level and the coupling from their own records (Section 6.7)	Its reading as the recovery defect of the dark sector, and the regional response that the Einstein theorem consumes.
What a reading leaves	Reading that a pair is present and reading where it is have the same first statistics and different later records (Section 6.6)	The tree of the presence reading is supplied apparatus.
Scalar channel	The scalar channel holds an object on four seams. Its excitation is kept for every interval, and after a pulse its seam record swings at one line, read from counts at 4.8990 of the observer's own reference and equal to the level difference read separately (Section 6.8)	A clock that starts with no supplied phase, and motion of the object: the level of a cage is flat.

11.1 The realization maps

Five maps specify physical identification independently of whether the finite mathematical result uses them.

(M1) Position and scale. A physical position and length for the carrier completion, compatible overlap gluing and a cofinal spatial refinement (Section 5).

(M2) Clock and energy calibration. One comparison between internal evolution, laboratory duration and measured energy. The calibrated reference clock and discrete native event counts are distinct.

(M3) Laboratory current. A physical gauge current and matter action with a continuum operator limit for the finite port response.

(M4) One common physical tower. One refinement family realizing the event, modular, stress, entropy, continuum, vacuum and scale premises together.

(M5) An implemented and matched action. A field and interaction law implemented by the same native services with complete states, relative normalizations and readouts. Declared architecture and empirical calibration are distinguished; physical propagation, currents and interactions must have compatible limits.

The finite constructions realize restricted instances of these maps. Their composition into the required physical theory does not follow from separate successful instances. A failure of a tested attachment rejects that attachment; a framework-wide rejection additionally requires a proof that it is forced.

12 Empirical meaning and falsifiability

The custody-bound register fixes target definitions, exclusion thresholds, precision floors, exposure classes and decision rules before eligible comparison [3]. Two kinds of test follow from the construction: a propagation anisotropy fixed by the carrier's symmetry, and an instrument test of the executable model. Published records also test precise attachments of committed records retrospectively.

12.1 Matches with nature

Structural results include the conditional Standard Model gauge Lie type and a declared matter representation with eight colour generators, one Higgs doublet, the generation charges and hypercharges, three colours and left-handed weak couplings. Finite results of the theory include a three-dimensional slow response and causal bounds, and the executable model adds bound objects that persist in the agreed records of its observers. Their domains and physical-identification conditions are stated separately. Table 13 retains the numerical comparisons, including their nonzero discrepancies. They are not a count of independent observational validations.

The coupling entries use the declared chain of the closure coordinates; its value of $1/\alpha$ is distinct from the pair scalar of Section 10.3. The primordial entries are conditional branch outputs and shared-data comparisons, without a joint independent likelihood. The capacity dictionary (31) gives the cosmological constant $1.096 \times 10^{-52}\,\mathrm{m}^{-2}$ against 1.089×10^{-52}, with the capacity chosen in view of the measured value, and the deep galaxy law gives the Tully–Fisher exponent 4 against 3.75 ± 0.09.

Table 13: Numerical comparisons. References include measurements and published bounds. Relative deviations alone do not establish agreement within experimental uncertainty. [a]Declared coupling chain of the closure coordinates [10]. [b]Against the joint ACT DR6, Planck and DESI chains the value lies in the lower 0.6 per cent tail (Section 12).

Quantity	**Source**	**Reference**	**Diff.**
$\alpha_s(m_Z)^a$	0.11834	0.1180(9)	+0.29%
$\sin^2\theta_W^a$	0.23074	0.23129(4)	−0.24%
$1/\alpha(m_Z)^a$	128.308	127.930(8)	+0.30%
$1/\alpha^a$	136.995	137.035999177(21)	−0.030%
n_s^b	0.9660	0.9649(42)	+0.12%
$dn_s/d\ln k$	0	−0.0045(67)	0.7σ
r	0	< 0.036	bound
Ω_K	0	0.0007(19)	0.4σ
$f_{\rm NL}$	0	−0.9(5.1)	0.2σ
Isocurvature	0	$< 2.5\%$	bound

12.2 Propagation anisotropy at angular rank six

Angular rank means spherical-harmonic rank j, not a particle spin. The dimension of the invariant subspace of the sixty proper icosahedral rotations in angular rank j is

$$m_j = \frac{1}{60}\Big[(2j+1) + 15\,U_{2j}(0) + 20\,U_{2j}(\tfrac{1}{2}) + 12\,U_{2j}(\tfrac{\varphi}{2}) + 12\,U_{2j}(\tfrac{\varphi-1}{2})\Big],$$

with U the Chebyshev polynomials of the second kind, and the exact table gives $m_1 = \cdots = m_5 = 0$ and $m_6 = 1$ [55].

Theorem 12.1 (Icosahedral angular-rank universality)**.** *Let the carrier kinetics be any operator $\lambda_a(k) = a^{-2}\sum_d w(d)\,[1-\cos(a\,k\cdot d)]$ with a finite direction multiset and weights invariant under the proper icosahedral rotation group. Then the dispersion is exactly isotropic through angular rank five at every order in a, every directional term below angular rank ten is one multiple of the unique normalized invariant $\mathcal{I}_6$, and whenever the weighted sixth-moment coefficient is nonzero the first directional artifact appears at order a^4k^6, suppressed by exactly $1/16$ under one binary refinement at that order. Rank six is the least symmetry-allowed nonzero anisotropic rank in the class.*

Proof. The order-$a^{2m-2}k^{2m}$ angular content is an invariant polynomial of degree $2m$ with harmonic components at even ranks $j \le 2m$, and the invariant table forces zero at $L = 2, 4, 8$ and a one-dimensional space at $L = 6$. The table, the 62-direction stationary census, the orbit verification and the nonvanishing sixth-moment coefficients are certified in exact arithmetic [1]. □

Proposition 12.2 (Primitive twelve-port branch prediction)**.** *Suppose the intrinsic spatial kinetic symbol lies in the cosine class of Theorem 12.1 with scale-independent coefficients, the complete orbit of the twelve port directions u_i is its sole hop support through order k^6, the carrier scale a is finite and positive with the quadratic term normalized to k^2, one carrier rest frame is transported coherently over the experiment, and the tested scalar or polarization-independent sector realizes the operator. Then*

$$\omega^2 = \frac{1}{2a^2}\sum_{i=1}^{12}[1-\cos(ak\,u_i\cdot\widehat{k})] = k^2 - \frac{a^2}{20}k^4 + \frac{a^4}{840}k^6 + \frac{2a^4}{7875}k^6\mathcal{I}_6(\widehat{k}) + O(a^6k^8), \tag{32}$$

with $\mathcal{I}_6(n) = \frac{25}{132}\sum_i P_6(u_i\cdot n)$*, so in a transported frame the branch predicts the scale-free relations*

$$\frac{B_6}{C_4^2} = \frac{32}{315}, \qquad \frac{B_0}{C_4^2} = \frac{10}{21}, \qquad \frac{B_6}{B_0} = \frac{16}{75}, \tag{33}$$

and every intrinsic anisotropic coefficient at $1 \le j \le 5$ *vanishes.*

Proof. The exact carrier moments $\sum_i (u_i\cdot n)^2 = 4$, $\sum_i (u_i\cdot n)^4 = 12/5$ and $\sum_i (u_i\cdot n)^6 = 12/7 + (64/175)\,\mathcal{I}_6(n)$ substituted into the cosine series give the expansion; eliminating a gives the ratios. □

A second frozen ray follows from the source seams.

Proposition 12.3 (Source-seam edge ray and conditional propagation branch)**.** *The boundary current of the complete thirty-seam source packet maps through the antipodal-odd load readout onto the even-sum module* D_6 *of Theorem 5.1, with Smith invariants* $(1,1,1,1,1,2)$*, and every directed seam defines one translation of the internal record carrier whose complete normalized direction multiset is the thirty-direction edge orbit. If the feasible move laws and their objective are natural under the proper carrier action and A3 supplies a unique normalized minimizer, transitivity forces weight* $1/60$ *on every directed seam, and the selected internal operator is the source-counting homogeneous convolution.*

Suppose these record translations are physical displacements under one homogeneous position action, that the complete edge orbit is the sole direct support through the displayed order, that proper-carrier covariance fixes one common weight, that the same operator acts on one scalar or polarization-independent physical sector with quadratic term normalized to k^2*, and that the action carries the stated gluing, scale, frame, readout, nuisance, and exclusivity data. Its spatial kinetic symbol is then*

$$\Lambda_a(k,\widehat{k}) = \frac{1}{5a^2}\sum_{j=1}^{30}\Big[1-\cos\Big(ak\,w_j\cdot\widehat{k}\Big)\Big], \tag{34}$$

with $C_4 = -a^2/20$*,* $B_0 = a^4/840$ *and* $B_6 = -a^4/12600$*, hence* $B_0/C_4^2 = 10/21$*,* $B_6/C_4^2 = -2/63$ *and* $B_6/B_0 = -1/15$*. The intrinsic anisotropic coefficients at angular ranks one through five vanish, and the rank-six vector lies on the rotated* $\mathcal{I}_6$ *orbit.*

Proof. Exact integer incidence gives the displayed image and Smith invariants, and the response-selected Gram pullback gives the completion of Theorem 5.1. The sixty directed labels map two-to-one onto the thirty signed edge directions, whose unit-normalized moments are $\sum_j (w_j\cdot n)^2 = 10$, $\sum_j (w_j\cdot n)^4 = 6$ and $\sum_j (w_j\cdot n)^6 = 30/7 - (2/7)\,\mathcal{I}_6(n)$; substitution in (34) gives the coefficients and ratios. The incidence, quotient, orbit binding and moment identities are machine-checked in exact arithmetic [1]. □

The proposition contains an exact finite source theorem and a conditional physical branch. The naturality and minimizer clause supplies a homogeneous internal action whose generator satisfies the positive maximum principle and an exact Dirichlet identity, and whose plane-wave spectrum is the symbol above. The edge branch and the primitive-port branch have opposite rank-six signs, and their coefficient rays, custody packages, exposure exclusions and comparison budgets are separate.

Theorem 12.4 (Carrier-class dispersion band)**.** *For the declared positive-weight scalar cosine class over orbits* O_s *of the sixty proper carrier rotations with radii* $r_s > 0$*, weights* $w_s > 0$ *and the* k^2 *coefficient normalized to one, write* $\Lambda_{\mathrm{norm}} = k^2 + C_4k^4 + (B_0 + B_6\mathcal{I}_6(\widehat{k}))k^6 + O(k^8)$ *and* $\mu_m = \sum_s w_s|O_s|r_s^m$*. Then* $C_4 = -(a^2/20)\mu_4/\mu_2 < 0$ *for every member;* $B_0/C_4^2 = (10/21)\mu_2\mu_6/\mu_4^2 \ge 10/21$

with equality exactly on single-radius members; the anisotropic ranks one through five vanish; and B_6/B_0 *lies in* $[-16/135, 16/75]$*, the face and vertex orbits attaining the endpoints and the edge orbit sitting at* $-1/15$*.*

Proof. Summing over the sixty rotations gives $\sum_g ((gu)\cdot\widehat{k})^6 = \frac{60}{7} + \frac{64}{35}\mathcal{I}_6(\widehat{u})\mathcal{I}_6(\widehat{k})$ on unit vectors. The floor is the Lagrange identity $\mu_2\mu_6 - \mu_4^2 = \sum_{i<j} W_i W_j r_i^2 r_j^2 (r_i^2 - r_j^2)^2 \geq 0$ with $W_s = w_s|O_s|$, and the band holds because the rank-six numerator is a positive-weighted mean of seed values of $\mathcal{I}_6$ in $[-5/9, 1]$ [1]. □

A resolved intrinsic dispersion with B_0/C_4^2 below $10/21$, or B_6/B_0 outside $[-16/135, 16/75]$, or a residue at ranks one through five, excludes every member of the declared class at once. The primitive-port relation is a frozen prospective conditional physical-branch prediction: its target statement, coefficient snapshot, registration record, public commit custody and detached calendar attestations fix the prospective content, the dated template search whose icosahedral templates returned a family-wide p-value of 0.64 is ineligible, and a verdict requires a dataset-specific registration with a joint likelihood, frames, orientation profile, nuisance model and calibrated threshold. The branch fails at five standard deviations or more if an isolated intrinsic C_4 is positive, a lower-rank coefficient is nonzero, or the calibrated profile likelihood excludes the complete manifold $C_4 < 0$, $B_0 = \frac{10}{21}C_4^2$, $B_6 = \frac{32}{315}C_4^2$. A null is inconclusive, since the branch supplies no positive lower bound on a, and a failure rejects the primitive twelve-port propagation branch; it reaches the framework as a whole only after a stronger source law makes that branch forced and exclusive [3].

12.3 An instrument test of the executable model

The executable model has two instrument tests: the particle-stability test of its seam interaction (Section 6.3) and the reunion test of the travelling clock of Interval Echo (Section 6.5). In the first, the instrument is the two-ended reader of every seam with its agreed record, the preparation is the local emitter, and the prediction is a probability law on the complete set of outcomes: one record for each seam and the outcome "no pair". Three outcomes count against the claim: "no pair" above the bound at a reading; in the audit of the spectrum, no level of two loads below the energy of two free loads; or a changed law with the same alphabet, routing and symmetry that gives the same answer on the whole property. None occurs in the runs. The exchange law alone loses the pair, and the law with the reversed sign keeps the pair and has no level below two free loads. The test compares distributions of observer records. It makes no statement about the encoding of the state, and the carrier on which it runs is hardware of the computation, no physical space. A comparison with what observers in our world record uses the effective description of Proposition 7.4 and the physical reading of the bound objects, whose requirements are listed in Section 11. In the second, the instrument is the shared seam on which both owners read their elapsed counts, the speeds come from the optics of the home observer, and the prediction is the forecast (18); a residual beyond its standard errors on a held journey counts against the clock.

12.4 Predictions of the model on records

Every result of the model is a probability of records under a stated preparation. Each is therefore a prediction for any realization of the model, on a quantum processor or in an independent simulation: the realization prepares, runs and reads as specified and compares its counts with Table 14, which names for each prediction the outcome that counts against it. A comparison with a laboratory system requires in addition that the same preparation, intervention and readout be identified in that system.

Table 14: Predictions of the model on records, and the outcome that counts against each.

Experiment	Prediction	Counts against it
A pair written on one seam, read later, $\kappa > 3$	"No pair" with probability at most $40/(2\kappa - 6)^2$ on every federation; at most 0.0097 at $\kappa = 8$ on 1 to 320 cells at the readings of Table 2	A larger probability at some reading
The same law without the agreement energy	"No pair" with probability up to 0.80 on 20 cells	A pair that is kept
Rounds of seam events in any order, with unequal rates of the observers	The pair is kept	A loss of the pair under rounds
Two readings of a pair, $\kappa = 8$, one cell	Equal first answers; later records that differ by more than 0.0817 in total variation; one event at 0.0183 against 0.1029	Equal laws of the later records
An unrecovered seam with empty ports	Read unrecovered at every reading; the rates of its two records return the coupling	A recovery; another ratio of the rates
The seam record of a cage after the coherent pulse	One line at $2\sqrt{6} = 4.8990$ of the observer's reference, with more than 0.9999 of the variance	A second line, or a line elsewhere
The fuel dial on the same cage	The level difference 4.8990, equal to the line	A value away from the line
The excitation of a cage after the sharp pulse	Read above 0.99 at waits of 0 to 512 steps, the same at every wait	A decrease with the wait
The cage under seam hopping round every port	No single line; the excitation is lost	A single line, or a kept excitation

12.5 Committed records against public data

Published records can test precise attachments of committed records without a new laboratory realization; the test below is retrospective, states its readout hypotheses, and assigns no prospective verdict.

The diagonal native branch is a classical stochastic process, so under independently chosen settings and local factorized responses it obeys the CHSH bound $S \leq 2$. The deposited records of the loophole-free Hensen experiment [79] reproduce 245 eligible trials, 196 wins and $S = 2.42250$, and the published fixed-count analysis gives a tail bound near 0.03917 with its setting-calibration allowance [77]. This rejects the local classical reading of the diagonal branch under that experimental contract. Committed native records form a classical process: the native grammar keeps diagonal inputs diagonal under every classical feedback history. Correlations beyond $S = 2$ therefore need uncommitted coherence from declared preparation services, and every admissible record law attenuates it [71]. The replay leaves the completed record surface untouched, on which a declared entangled state reaches the Tsirelson bound of Theorem 4.5, and it does not distinguish C from E.

12.6 Diagnostics and what fails together

The other quantitative comparisons carry their own decision shapes and do not count as predictions. The closure roots of Section 10.3 are diagnostics of declared maps. The registered conditional primordial branch $n_s = 1 - P/48 = 0.96602$, at the calibrated grain P, lies at the lower 0.612 percent position of the official ACT DR6, Planck and DESI joint posterior chains, whose mean

is 0.9743 ± 0.0034 [80, 78]. Those data precede the registration, so this is a retrospective tension under baseline ΛCDM, not a likelihood ratio, and the registered comparison with a later dataset is unchanged. A resolved deep-regime galaxy sample violating degree-one radial scale covariance or quadrature composition removes the uniqueness of the deep law, and exclusion of $(w_0, w_a) = (-1, 0)$ fails the fixed-capacity branch. The conditional implications share premises, so they fail in groups: failure of (M4) removes the effective-spacetime and Einstein conclusions together, failure of (M3) removes the gauge and matter interpretations together, and failure of (M2) removes every statement in laboratory units. The finite normal-form, invariant-theory and algebraic results retain their stated domains under all three.

13 Machine verification and reproducibility

Each result is identified by its artifact as a Lean theorem, exact executable certificate, conditional paper argument, numerical receipt, or explicit unproved premise. A finite theorem is a deduction from stated premises on a specified domain. An exhaustive certificate belongs to that proof only when its enumeration and soundness argument are supplied. Exact executable certificates recompute integer or rational identities and outward error bounds; numerical receipts retain their declared tolerances. A conditional analytic theorem consumes a specified continuum object, whereas a source limit theorem derives a limit from a declared execution family with explicit normalization and error control. Neither establishes its own physical identification. Reconstruction implications retain their geometric premises and unsupplied realization maps.

Calibration consumes comparison data. A prospective conditional test fixes its observable, precision, decision rule and source before an eligible comparison; a frozen branch prediction additionally identifies which physical branch the result can reject. These distinctions apply to each numerical comparison and prevent the same supplied target from being counted as independent evidence.

The Lean dependency closures reported here contain no admitted propositions. The executable certificates bind their source, inputs and full outcomes, including failed preparation and complementary sectors. Independent replay checks canonical exact outputs and the stated numerical tolerances, while adversarial tests exercise the acceptance boundaries. For the contrast-memory seam, the reduction of Proposition 3.4 is checked in exact symbolic arithmetic on all 99 local states, the constants of Theorem 6.1 are recomputed on the federations of 20, 80 and 320 cells, and the particle-stability test is rerun under changed laws. For Interval Echo, the reunion cohorts, the bulk agreement records and the current closure are replayed from their seeds.

The source, receipts and rebuild commands are public [1, 2, 68]. The executable-model paper gives the specification, the proofs and the resources of the candidate laws [67]; the source-limit document states convergence constants and orders of limits [73]. Public-data reducers bind their datasets, observation hypotheses and decision rules [77, 78]. Exact finite certificates, analytic limit proofs and physical comparisons retain these distinct domains throughout the paper.

14 Discussion and comparison

Operational reconstructions derive quantum structure from information and composition principles [22, 23, 24]. OPH makes a narrower statement at the quantum stage: it takes the finite algebra-state representation as an input and contributes the completed-record surface on which the event, conditioning and correlation identities operate, together with the consensus theorem that defines completion and a positive functional reconstructed from native repair histories. Quantum Darwinism locates classical objectivity in redundant environmental records [50], and the completed-consensus

record plays the same public role with redundancy replaced by protected overlap agreement and an explicit repair dynamics. The cellular-automaton programme shares the finite substrate [51], while OPH locates the quantum identities on the completed record surface. Wigner's-friend extensions constrain agents reasoning about one another's unfinished measurements [52], whose premises concern pre-consensus perspectives that the completed surface does not represent. Relational quantum mechanics treats physical facts as relational [48] and the thermal-time programme reads time from modular structure [49]; OPH attaches public facts to protected overlap records and treats modular flow as state- and event-relative. The local-diamond proof sits beside asynchronous agreement [44, 45], and Dijkstra's self-stabilization separates recovery from continued legitimate operation [46].

The gravitational branch belongs to the thermodynamic and entanglement-based routes to geometry [59, 60, 63], with Bisognano–Wichmann modular flow and half-sided modular inclusions as established analytic ingredients [56, 57, 58]. The route from a null-projected balance and the Bianchi identity to the full equation, with Λ as an integration constant, is familiar from trace-free and unimodular formulations [61, 62]; what is added is the finite nine-direction design with exact constants and the premise contract (G1)–(G6) stated as one implication. The gauge section uses Doplicher–Roberts reconstruction for the sector group [65, 66] and contributes the forcing of the local Lie type from complete response and rechartings inner on that response, a stronger premise than mere internal availability of their implementers.

The closure hypothesis has precedents of a different kind. Wheeler pictured a participatory universe as a self-excited circuit [85]. Tegmark's mathematical-universe hypothesis identifies physical existence with mathematical structure [86], and Nozick proposed that a fundamental principle might subsume itself [87]. OPH adds two demands: the self-subsumption must be inhabited, carried out through records and agents inside the structure, and it must be testable in part, through an executable specification whose observers can be run and whose instruments make predictions. Lawvere's fixed-point theorem shows why unrestricted self-representation fails [88]; the closure condition is restricted to the observable and interventional structure that observers can recover.

The characteristic test of this proposal is an intervention whose record can be predicted in two descriptions. A pulse routed through finite port memories can also be described as a wave travelling between stations. The chart recovered from the first measurements predicts where subsequent pulses arrive. A source of gravity would have to pass a stronger test. The stress assigned to a matter preparation would have to predict curvature measured by an independent observer, with the same coupling for different sources. The semiclassical comparison in Section 9 gives an example in which this test succeeds and detects a deliberate change of coupling.

15 Conclusion

A field in spacetime can describe measurements made inside a computation specified by finite registers and local operations. In the scalar experiment, the wiring and the clocked pulse sequence are explicit. An observer with access to station records recovers three coordinates, predicts the held arrivals and can describe the prescribed refinement by a relativistic free field. On the same hardware the pair instruments distinguish two quantum state updates, the current pulses have detectable effects and a signed defect transports a coherent orbital state. The rotation and exchange tests in Section 8.4 identify the orbital character of that state. The written-field extension supplies a candidate charge and field response. Identifying an electron requires the charge, spin and rest energy of one freely travelling excitation.

The finite theorems constrain what observers can recover. Under their respective hypotheses,

repair fixes a public normal form and additive probabilities on effects fix a density matrix. A complete compact response that implements cell rotations internally fixes the gauge Lie type. For gravity the corresponding implication is from fixed-proper-volume entropy stationarity and its geometric normalization to null balance, and from null balance and conserved stress to the Einstein equation. Realizing those hypotheses on one freely evolving material would make the gravitational law a consequence of the observers' consistency conditions. The independent geometric test on that material is to predict radar or proper area from its measured matter stress.

The closure question turns this reconstruction back on the observers. If a history contains the discovery of its own specification and the construction of hardware that realizes it, then the making of that hardware is itself an event in the history it realizes. The finite packet theorem supplies an explicit fixed-point map, and the local recovery experiment supplies a specification that can be run again. The physical claim concerns the complete history. An internal realization must reproduce its observers' joint responses to intervention, including observations by which our Universe can be distinguished from other admissible histories.

Reproducibility statement

All theorems, certificates, simulation configurations, receipts, and the formal library are public in the project repositories [1, 2], and the executable model with its candidate laws and their tests is in the same repository [68]. The paper release manifest records the release identifier (r2073) with PDF hashes and sizes; computational receipt bundles pin the applicable source revision, configuration, seed and output hashes, with clean-checkout rebuild instructions and negative controls; and machine-readable claim and prediction provenance accompanies the artifacts [3]. This manuscript synthesizes and strengthens results whose longer proofs also appear in public component preprints on observable normal forms, finite event algebras, consensus, Einstein reconstruction, gauge structure and the executable observer [4, 5, 6, 9, 11, 67], a relationship disclosed here so that overlap is visible.

Statements and Declarations

Funding. The authors declare that no external grants or dedicated third-party research funding were received for the preparation of this manuscript.

Author contributions. Bernhard Mueller developed the OPH concept and mathematical synthesis, wrote the main manuscript, and coordinated the formal and computational evidence. Mario Poneder developed executable observer constructions and their certificates, among them the register form and local preparation of the scalar channel, the finite clock and the pair-presence instrument of A-contrast-memory-spherical-v1, and contributed the finite port-current construction and verifier, gauge and matter certificates, and proof review of the edge-entropy and Einstein-normalization branches. Alexander Osika proposed that the screen pixel ratio and the correctable-record capacity are derivable rather than fitted, supplied the detuning fixed-point equation that determines the pixel ratio, and originated the echosahedral patch-hardware design on which the screen-microphysics branch is built, in addition to the physical-realization and hardware boundary, prototype framing, and manuscript review. Kai Xue contributed consistency checks, simulator review, visualization review, and prototype-engineering review. Ben Cassie contributed implementation-claim and physical-evidence review. Peter Nguyen contributed proof auditing, branch-boundary analysis, compact-gauge and global-quotient analysis, and manuscript consistency review. Jinwook Kim developed the constructions, proofs, and counterexamples for the profile partition and struc-

tural characterizations, exact behavior-cut recovery, exact finite-state profile transport, adaptive repair stratification, the cumulative attempt-capacity classification, fixed computation-federation progress, and the fixed-federation execution classification, together with the mechanism-variant comparison kernel and conditional example and the source-derived phase-effect selection. He constructed a provably fair emission-order round-robin scheduler with a linear exact-output attempt bound, established order-sharp quadratic accepted-step bounds for the actual compiler with the exponential fanout control, and proved the historical weak-relation fair-stuttering no-go and the weak-fair delay versus bounded-waste horizon separation. He formalized these results in Lean, connected the repair and execution results to the Tower library, and contributed their manuscript, claim registry, ledger and build records. David Matscheko contributed proof review of consensus repair, observable normal forms, modular and Einstein algebra, edge entropy, hypercharge, and the $\mathbb{Z}_6$ quotient. Daniel Ari Friedman contributed independent red-team audits of the papers, the book, the claim and premise ledgers, the Lean library, continuous integration and the custody records, which led to scoped headline claims, displayed values matched to their certified receipts and repaired falsification rules, and the independently reviewed programme-obstruction audit whose controls bound how the carrier, the response triplets, the feedback class and the kinetic term may be attached. Jonathan Hill contributed Lean formalization and proof auditing of observable normal forms, refinement and repair results, complexity classifications, and artifact coverage. William T. Glynn contributed simulator development, computational implementation, reproducible-build infrastructure, and release-validation work in the main OPH research repository. Maarten Antonie Visser contributed consensus-protocol review, physics feedback on the foundations and emergent-spacetime framing, and the source-derived causal-poset reading of authenticated provenance that the event-precedence layer implements. Kale Arnav Anirudha contributed consensus-paper material, asynchronous-agreement analysis, repair-map definitions, and formal review of the protocol surface. Brieuc de La Fournière contributed finite Lean constructions on the source-derived causal-order and carrier-symmetry surfaces, including the cover-relation provenance compiler and the antipodal port-action identification, and external comparison controls for the charged-lepton branch. All authors reviewed and approved the manuscript. All authors agree to be accountable for all aspects of the work.

Corresponding author. Correspondence should be addressed to Bernhard Mueller.
Email: `bernhard@floatingpragma.ai`.

Data availability. The finite witnesses, simulation configurations, receipts, scientific claim registries, and release manifests supporting this study are available in the public OPH and simulation repositories [1, 2]. Individual receipts and their bundle documentation provide the source and output provenance for computational claims. The artifact map identifies the level-six exact-federation archive and its level-five to level-ten extension, the closure-loop archive, and the causal-poset archive.

Code availability. The Lean sources, exact-arithmetic verifiers, finite scans, simulation code, tests, and rebuild instructions are available in the same public repositories [1, 2]. The computational claims in this manuscript identify their principal files in Section 13.

Ethics approval and consent to participate. Not applicable. The study involved no human participants, human data, or animals.

Consent for publication. Not applicable.

Competing interests. The authors participate in OPH-related research, software, simulation, or prototype-development programs and may receive professional or reputational benefit from this work. These relationships are disclosed. The authors declare no other competing interests.

Credited prior work

The results of this paper build on the following established work. Each entry names an established result as it is used here and cites its sources.

- Icosahedral harmonics, finite-difference dispersion, and nonminimal Standard-Model Extension coefficient searches [96, 98, 94, 95].
- Root lattices, graph incidence, transverse projectors, free-vector oscillators, icosahedral edge harmonics, finite-difference symbols, Lorentz-violating threshold kinematics, and nonminimal Standard-Model Extension coefficient searches [90, 92, 99, 97, 93, 94, 95].
- Spherical-design moment theory, lattice dispersion expansions, and Lorentz-violation coefficient parametrizations [91, 97, 94, 89].

References

[1] FloatingPragma (2026). Observer Patch Holography: Lean library, exact code receipts, finite certificates, and scientific claim registries. https://github.com/FloatingPragma/observer-patch-holography

[2] Mueller, B. (2026). OPH physics simulator and reproduction source. https://github.com/muellerberndt/oph-physics-sim. Exact-federation archive: https://github.com/FloatingPragma/observer-patch-holography/tree/r2073/evidence/exact_federation_L6_canonical_20260909. Closure-loop archive: https://github.com/FloatingPragma/observer-patch-holography/tree/r2073/evidence/closure_loop. Causal-poset archive: https://github.com/FloatingPragma/observer-patch-holography/tree/r2073/evidence/source_net_causal_poset. Active refinement-readout revision: https://github.com/muellerberndt/oph-physics-sim/tree/036b12b608a9ca4c19d69f5e951b3b83a7a51cd8.

[3] FloatingPragma (2026). Precommitted comparison certificates, custody records, and the frozen prediction register. Immutable source receipt: https://github.com/FloatingPragma/observer-patch-holography/blob/66176656dc1143f9ec50ba1a6e409c403545857f/code/a5_fingerprint/runtime/spin_six_primitive_port_prediction_receipt.json. Append-only custody packet: https://github.com/FloatingPragma/observer-patch-holography/tree/bb73f80d459113ccc82d5a5b5219d1dda78e9a79/evidence/custody/falsification/frozen_targets/fz11_2026-07-31. Source-seam edge receipt: https://github.com/FloatingPragma/observer-patch-holography/blob/r2073/code/a5_fingerprint/runtime/seam_current_edge_prediction_receipt.json. Source-seam custody and decision-rule clarification: https://github.com/FloatingPragma/observer-patch-holography/tree/bb73f80d459113ccc82d5a5b5219d1dda78e9a79/evidence/custody/falsification/frozen_targets/fz12_2026-08-02. Live register: https://github.com/FloatingPragma/observer-patch-holography/blob/r2073/claims/frozen_prediction_register.json.

[4] Mueller, B., Kim, J., Matscheko, D., and Hill, J. (2026). *Observation-Determined Normal Forms: Stability, Obstructions, and Refinement in Constraint and Rewrite Systems*. Public manuscript in the same repository revision as this paper. https://github.com/FloatingPragma/observer-patch-holography/blob/r2073/extra/observable_normal_forms.pdf

[5] Mueller, B. (2026). *Verified Projection-Event Calculus in Lean 4: Bundled Arbitrary-Partition Pinching, Lüders Retractions, and CHSH Interoperability*. Public manuscript and formal artifact. https://github.com/FloatingPragma/observer-patch-holography/blob/r2073/extra/machine_checked_finite_event_algebras.pdf

[6] Mueller, B., Xue, K., Kim, J., Anirudha, K. A., Matscheko, D., and Hill, J. (2026). *Reality as a Consensus Protocol: The Fixed-Point Computation That Implements Physics*. Public manuscript. https://github.com/FloatingPragma/observer-patch-holography/blob/r2073/paper/reality_as_consensus_protocol.pdf

[7] Mueller, B., Osika, A., Xue, K., Cassie, B., de La Fournière, B., and Friedman, D. A. (2026). *Twelve-Port Icosahedral Carriers and Native Seam Repair: The Carrier Layer of Observer Patch Holography*. Public manuscript. https://github.com/FloatingPragma/observer-patch-holography/blob/r2073/paper/screen_microphysics_and_observer_synchronization.pdf

[8] Mueller, B., Poneder, M., Osika, A., Xue, K., Cassie, B., Nguyen, P., and Friedman, D. A. (2026). *Observers Are All You Need*. Public manuscript. https://github.com/FloatingPragma/observer-patch-holography/blob/r2073/paper/observers_are_all_you_need.pdf

[9] Mueller, B., Poneder, M., Osika, A., Xue, K., Nguyen, P., Visser, M. A., Matscheko, D., and de La Fournière, B. (2026). *Recovering Observer Spacetime and Einstein Dynamics from Overlap Consistency*. Public manuscript. https://github.com/FloatingPragma/observer-patch-holography/blob/r2073/paper/recovering_observer_spacetime_and_einstein_dynamics_from_overlap_consistency.pdf

[10] Mueller, B., Osika, A., and Friedman, D. A. (2026). *The Fine-Structure Constant as an OPH Pixel Fixed Point*. Public manuscript. https://github.com/FloatingPragma/observer-patch-holography/blob/r2073/extra/fine_structure_constant_derivation.pdf

[11] Mueller, B., Poneder, M., Osika, A., Xue, K., Nguyen, P., Matscheko, D., and Friedman, D. A. (2026). *Standard Model Gauge Structure under Complete-Response and Observer-Transport Premises*. Public manuscript. https://github.com/FloatingPragma/observer-patch-holography/blob/r2073/paper/deriving_standard_model_gauge_structure_from_observer_overlap_consistency.pdf

[12] Mueller, B., Poneder, M., Osika, A., Xue, K., and Friedman, D. A. (2026). *Particles from Observer Consistency: Defect Classes, Statistics and the Bound Objects of an Executable Observer*. Public manuscript. https://github.com/FloatingPragma/observer-patch-holography/blob/main/paper/deriving_the_particle_zoo_from_observer_consistency.pdf

[13] Mueller, B. (2026). *The de Sitter Time-Advance Sign from a Finite Screen with Fixed Capacity*. Public manuscript. https://github.com/FloatingPragma/observer-patch-holography/blob/r2073/extra/de_sitter_time_advance_sign_from_fixed_screen_capacity.pdf

[14] Mueller, B. and Matscheko, D. (2026). *Observer Patch Holography and the Dark Sector: Modular Charge, the Anomalous Collar Source, and the Deep Galaxy Law*. Public manuscript. https://github.com/FloatingPragma/observer-patch-holography/blob/r2073/cosmology/oph_dark_matter_paper.pdf

[15] Mueller, B. (2026). *Observer Patch Holography Cosmological Vacuum and Structure Formation: Finite Transfer Conditions, Fluctuation Ensembles, and Proto-Objects*. Public manuscript. https://github.com/FloatingPragma/observer-patch-holography/blob/r2073/cosmology/oph_cosmological_vacuum_and_structure_formation.pdf

[16] Mueller, B. (2026). *Observer-Screen Synchronization as a Candidate Inflation-Free Branch: Record-Density Expansion, Required Premises and a Conditional Tilt*. Public manuscript. https://github.com/FloatingPragma/observer-patch-holography/blob/main/cosmology/oph_inflation_without_inflaton_observer_screen_synchronization.pdf

[17] Mueller, B. (2026). *A Finite Black-Hole Information Ledger for Observer Patch Holography*. Public manuscript. https://github.com/FloatingPragma/observer-patch-holography/blob/main/cosmology/oph_black_hole_information_ledger.pdf

[18] Wissner-Gross, A. D. (2026). *A Parameter-Free Candidate for the Fine-Structure Constant from Entangled Qudits*. Preprint. https://alexwg.org/publications/ChainTheoryAlpha.pdf

[19] Mohr, P. J., Newell, D. B., Taylor, B. N., and Tiesinga, E. (2025). CODATA recommended values of the fundamental physical constants: 2022. *Reviews of Modern Physics* **97**, 025002.

[20] Mueller, B. and Hill, J. (2026). *A Conditional Identification of the Yang–Mills Gap with a Finite Repair Gap: Dobrushin Repair Floors and a $\mathbb{Z}_2$ Test of the Transfer Receipt*. Public manuscript. https://github.com/FloatingPragma/observer-patch-holography/blob/r2073/extra/yang_mills_gap_clay_problem.pdf

[21] Einstein, A., Podolsky, B., and Rosen, N. (1935). "Can quantum-mechanical description of physical reality be considered complete?" *Physical Review* **47**, 777–780. https://doi.org/10.1103/PhysRev.47.777

[22] Hardy, L. (2001). "Quantum theory from five reasonable axioms." arXiv:quant-ph/0101012. https://arxiv.org/abs/quant-ph/0101012

[23] Chiribella, G., D'Ariano, G. M., and Perinotti, P. (2011). "Informational derivation of quantum theory." *Physical Review A* **84**, 012311. https://doi.org/10.1103/PhysRevA.84.012311

[24] Masanes, L., and Müller, M. P. (2011). "A derivation of quantum theory from physical requirements." *New Journal of Physics* **13**, 063001. https://doi.org/10.1088/1367-2630/13/6/063001

[25] Gleason, A. M. (1957). "Measures on the closed subspaces of a Hilbert space." *Journal of Mathematics and Mechanics* **6**, 885–893.

[26] Boyd, G., Engels, J., Karsch, F., Laermann, E., Legeland, C., Lütgemeier, M., and Petersson, B. (1996). "Thermodynamics of SU(3) lattice gauge theory." *Nuclear Physics B* **469**, 419–444. https://arxiv.org/abs/hep-lat/9602007

[27] Busch, P. (2003). "Quantum states and generalized observables: A simple proof of Gleason's theorem." *Physical Review Letters* **91**, 120403. https://doi.org/10.1103/PhysRevLett.91.120403

[28] Clauser, J. F., Horne, M. A., Shimony, A., and Holt, R. A. (1969). "Proposed experiment to test local hidden-variable theories." *Physical Review Letters* **23**, 880–884. https://doi.org/10.1103/PhysRevLett.23.880

[29] Cirel'son, B. S. (1980). "Quantum generalizations of Bell's inequality." *Letters in Mathematical Physics* **4**, 93–100. https://doi.org/10.1007/BF00417500

[30] Landau, L. J. (1987). "On the violation of Bell's inequality in quantum theory." *Physics Letters A* **120**, 54–56. https://doi.org/10.1016/0375-9601(87)90075-2

[31] Wootters, W. K., and Zurek, W. H. (1982). "A single quantum cannot be cloned." *Nature* **299**, 802–803. https://doi.org/10.1038/299802a0

[32] Dieks, D. (1982). "Communication by EPR devices." *Physics Letters A* **92**, 271–272. https://doi.org/10.1016/0375-9601(82)90084-6

[33] Lüders, G. (1950). "Über die Zustandsänderung durch den Meßprozeß." *Annalen der Physik* **443**, 322–328. https://doi.org/10.1002/andp.19504430510

[34] Bombelli, L., Lee, J., Meyer, D., and Sorkin, R. D. (1987). "Space-time as a causal set." *Physical Review Letters* **59**, 521–524. https://doi.org/10.1103/PhysRevLett.59.521

[35] Surya, S. (2019). "The causal set approach to quantum gravity." *Living Reviews in Relativity* **22**, 5. https://doi.org/10.1007/s41114-019-0023-1

[36] Major, S., Rideout, D., and Surya, S. (2007). "On recovering continuum topology from a causal set." *Journal of Mathematical Physics* **48**, 032501. https://doi.org/10.1063/1.2435599

[37] Myrheim, J. (1978). "Statistical geometry." CERN preprint TH-2538.

[38] Meyer, D. A. (1988). "The Dimension of Causal Sets." PhD thesis, Massachusetts Institute of Technology.

[39] Benincasa, D. M. T., and Dowker, F. (2010). "The scalar curvature of a causal set." *Physical Review Letters* **104**, 181301. https://doi.org/10.1103/PhysRevLett.104.181301

[40] Dowker, F., and Glaser, L. (2013). "Causal set d'Alembertians for various dimensions." *Classical and Quantum Gravity* **30**, 195016. https://doi.org/10.1088/0264-9381/30/19/195016

[41] Hawking, S. W., King, A. R., and McCarthy, P. J. (1976). "A new topology for curved space–time which incorporates the causal, differential, and conformal structures." *Journal of Mathematical Physics* **17**, 174–181. https://doi.org/10.1063/1.522874

[42] Malament, D. B. (1977). "The class of continuous timelike curves determines the topology of spacetime." *Journal of Mathematical Physics* **18**, 1399–1404. https://doi.org/10.1063/1.523436

[43] Lamport, L. (1978). "Time, clocks, and the ordering of events in a distributed system." *Communications of the ACM* **21**(7), 558–565. https://doi.org/10.1145/359545.359563

[44] Lamport, L., Shostak, R., and Pease, M. (1982). "The Byzantine generals problem." *ACM Transactions on Programming Languages and Systems* **4**(3), 382–401. https://doi.org/10.1145/357172.357176

[45] Fischer, M. J., Lynch, N. A., and Paterson, M. S. (1985). "Impossibility of distributed consensus with one faulty process." *Journal of the ACM* **32**(2), 374–382. https://doi.org/10.1145/3149.214121

[46] Dijkstra, E. W. (1974). "Self-stabilizing systems in spite of distributed control." *Communications of the ACM* **17**(11), 643–644. https://doi.org/10.1145/361179.361202

[47] Newman, M. H. A. (1942). "On theories with a combinatorial definition of equivalence." *Annals of Mathematics* **43**(2), 223–243. https://doi.org/10.2307/1968867

[48] Rovelli, C. (1996). "Relational quantum mechanics." *International Journal of Theoretical Physics* **35**, 1637–1678. https://doi.org/10.1007/BF02302261

[49] Connes, A., and Rovelli, C. (1994). "Von Neumann algebra automorphisms and time-thermodynamics relation in generally covariant quantum theories." *Classical and Quantum Gravity* **11**, 2899–2917. https://doi.org/10.1088/0264-9381/11/12/007

[50] Zurek, W. H. (2003). "Decoherence, einselection, and the quantum origins of the classical." *Reviews of Modern Physics* **75**, 715–775. https://doi.org/10.1103/RevModPhys.75.715

[51] 't Hooft, G. (2016). *The Cellular Automaton Interpretation of Quantum Mechanics*. Fundamental Theories of Physics 185. Springer, Cham. https://doi.org/10.1007/978-3-319-41285-6

[52] Frauchiger, D., and Renner, R. (2018). "Quantum theory cannot consistently describe the use of itself." *Nature Communications* **9**, 3711. https://doi.org/10.1038/s41467-018-05739-8

[53] Ratcliffe, J. G. (2019). *Foundations of Hyperbolic Manifolds*, 3rd ed. Graduate Texts in Mathematics 149. Springer, Cham. https://doi.org/10.1007/978-3-030-31597-9

[54] Serre, J.-P. (1977). *Linear Representations of Finite Groups*. Graduate Texts in Mathematics 42. Springer, New York. https://doi.org/10.1007/978-1-4684-9458-7

[55] Cohan, N. V. (1958). "The spherical harmonics with the symmetry of the icosahedral group." *Proceedings of the Cambridge Philosophical Society* **54**(1), 28–38. https://doi.org/10.1017/S0305004100033156

[56] Bisognano, J. J., and Wichmann, E. H. (1975). "On the duality condition for a Hermitian scalar field." *Journal of Mathematical Physics* **16**, 985–1007. https://doi.org/10.1063/1.522605

[57] Bisognano, J. J., and Wichmann, E. H. (1976). "On the duality condition for quantum fields." *Journal of Mathematical Physics* **17**, 303–321. https://doi.org/10.1063/1.522898

[58] Wiesbrock, H.-W. (1993). "Half-sided modular inclusions of von Neumann algebras." *Communications in Mathematical Physics* **157**, 83–92. https://doi.org/10.1007/BF02098019

[59] Jacobson, T. (1995). "Thermodynamics of spacetime: The Einstein equation of state." *Physical Review Letters* **75**, 1260–1263. https://doi.org/10.1103/PhysRevLett.75.1260

[60] Jacobson, T. (2016). "Entanglement equilibrium and the Einstein equation." *Physical Review Letters* **116**, 201101. https://doi.org/10.1103/PhysRevLett.116.201101

[61] van der Bij, J. J., van Dam, H., and Ng, Y. J. (1982). "The exchange of massless spin-two particles." *Physica A* **116**, 307–320. https://doi.org/10.1016/0378-4371(82)90247-3

[62] Ellis, G. F. R., van Elst, H., Murugan, J., and Uzan, J.-P. (2011). "On the trace-free Einstein equations as a viable alternative to general relativity." *Classical and Quantum Gravity* **28**, 225007. https://doi.org/10.1088/0264-9381/28/22/225007

[63] Van Raamsdonk, M. (2010). "Building up spacetime with quantum entanglement." *General Relativity and Gravitation* **42**, 2323–2329. https://doi.org/10.1007/s10714-010-1034-0

[64] Hall, B. C. (2015). *Lie Groups, Lie Algebras, and Representations: An Elementary Introduction*, 2nd ed. Graduate Texts in Mathematics 222. Springer, Cham. https://doi.org/10.1007/978-3-319-13467-3

[65] Doplicher, S., and Roberts, J. E. (1989). "A new duality theory for compact groups." *Inventiones Mathematicae* **98**, 157–218. https://doi.org/10.1007/BF01388849

[66] Doplicher, S., and Roberts, J. E. (1990). "Why there is a field algebra with a compact gauge group describing the superselection structure in particle physics." *Communications in Mathematical Physics* **131**, 51–107. https://doi.org/10.1007/BF02097680

[67] Mueller, B., Poneder, M., Kim, J., and Friedman, D. A. (2026). *An Executable Observer for Observer Patch Holography: Specification, Memory and Agreed Records.* Public manuscript. https://github.com/FloatingPragma/observer-patch-holography/blob/r2073/paper/executable_observer_construction.pdf

[68] FloatingPragma (2026). The executable model: the fixed spherical federation, the candidate laws Interval Echo, A-contrast-memory-spherical-v1 and the scalar channel, and their evaluation. https://github.com/FloatingPragma/observer-patch-holography/tree/r2073/model

[69] Nachtergaele, B., and Starr, S. (2001). "Droplet states in the XXZ Heisenberg chain." *Communications in Mathematical Physics* **218**. arXiv:math-ph/0009002. https://doi.org/10.1007/s002200100421

[70] Fischbacher, C., and Stolz, G. (2018). "Droplet states in quantum XXZ spin systems on general graphs." *Journal of Mathematical Physics* **59**, 051901. arXiv:1712.10276. https://doi.org/10.1063/1.5023216

[71] FloatingPragma (2026). Admissible record laws for native repair. https://github.com/FloatingPragma/observer-patch-holography/blob/r2073/model/record_laws/README.md

[72] FloatingPragma (2026). Native quantum mixing and the full-carrier memory boundary. https://github.com/FloatingPragma/observer-patch-holography/blob/r2073/model/observer/QUANTUM_MIXING.md

[73] FloatingPragma (2026). A spatial fluctuation field from one native history: the common spatial generator, its locality and spectral dimension, and the boundary-trace test. https://github.com/FloatingPragma/observer-patch-holography/blob/r2073/model/physical_space_time/OCCUPATION_FIELD.md

[74] FloatingPragma (2026). Joint time and field laws on matched source screens. https://github.com/FloatingPragma/observer-patch-holography/blob/r2073/model/observer_time_fields/REFINEMENT.md

[75] FloatingPragma (2026). Tangent first laws and finite entropy changes: native reference entropy and region boundaries. https://github.com/FloatingPragma/observer-patch-holography/blob/r2073/code/geometry/ENTROPY_FIRST_LAW_AUDIT.md

[76] FloatingPragma (2026). Exact native causal cones. https://github.com/FloatingPragma/observer-patch-holography/blob/r2073/model/common_source/CAUSALITY.md

[77] FloatingPragma (2026). Classical record responses and published Bell measurements. https://github.com/FloatingPragma/observer-patch-holography/blob/r2073/model/predictions/BELL_RECORDS.md

[78] FloatingPragma (2026). OPH predictions and public-data comparisons. https://github.com/FloatingPragma/observer-patch-holography/blob/r2073/docs/research/PUBLIC_DATA_PREDICTION_AUDIT.md

[79] Hensen, B. et al. (2015). Loophole-free Bell inequality violation using electron spins separated by 1.3 kilometres. *Nature* 526, 682–686. https://doi.org/10.1038/nature15759

[80] Louis, T. et al. (2025). The Atacama Cosmology Telescope: DR6 power spectra, likelihoods and ΛCDM parameters. arXiv:2503.14452. https://arxiv.org/abs/2503.14452

[81] Mosco, U. (1994). Composite media and asymptotic Dirichlet forms. *J. Funct. Anal.* 123, 368–421.

[82] Fukushima, M., Oshima, Y. and Takeda, M. (2011). *Dirichlet Forms and Symmetric Markov Processes*, 2nd edition. De Gruyter, Berlin.

[83] Coulhon, T. and Sikora, A. (2008). Gaussian heat kernel upper bounds via the Phragmén–Lindelöf theorem. *Proc. London Math. Soc.* 96, 507–544.

[84] FloatingPragma (2026). *The OPH Basis*: the closure hypothesis, the no-outside rule, the agreement condition, the executable specification, and the theorem-library premises. https://github.com/FloatingPragma/observer-patch-holography/blob/r2073/claims/axiom_registry.yaml

[85] Wheeler, J. A. (1983). "Law without law." In J. A. Wheeler and W. H. Zurek (eds.), *Quantum Theory and Measurement*, 182–213. Princeton University Press.

[86] Tegmark, M. (2008). "The mathematical universe." *Foundations of Physics* **38**, 101–150. https://doi.org/10.1007/s10701-007-9186-9

[87] Nozick, R. (1981). *Philosophical Explanations*. Harvard University Press.

[88] Lawvere, F. W. (1969). "Diagonal arguments and cartesian closed categories." *Lecture Notes in Mathematics* **92**, 134–145. https://doi.org/10.1007/BFb0080769

[89] Colladay, D., and Kostelecký, V. A. (1998). "Lorentz-violating extension of the standard model." *Physical Review D* **58**, 116002. https://doi.org/10.1103/PhysRevD.58.116002

[90] Conway, J. H., and Sloane, N. J. A. (1999). *Sphere Packings, Lattices and Groups*. Springer New York. https://doi.org/10.1007/978-1-4757-6568-7

[91] Delsarte, P., Goethals, J. M., and Seidel, J. J. (1977). "Spherical codes and designs." *Geometriae Dedicata* **6**, 363–388. https://doi.org/10.1007/BF03187604

[92] Godsil, C., and Royle, G. (2001). *Algebraic Graph Theory*. Springer. https://doi.org/10.1007/978-1-4613-0163-9

[93] Jacobson, T., Liberati, S., and Mattingly, D. (2003). "Threshold effects and Planck scale Lorentz violation: Combined constraints from high energy astrophysics." *Physical Review D* **67**, 124011. https://doi.org/10.1103/PhysRevD.67.124011

[94] Kostelecký, V. A., and Mewes, M. (2009). "Electrodynamics with Lorentz-violating operators of arbitrary dimension." *Physical Review D* **80**, 015020. https://doi.org/10.1103/PhysRevD.80.015020

[95] Kostelecký, V. A., and Russell, N. (2011). "Data tables for Lorentz and CPT violation." *Reviews of Modern Physics* **83**, 11–31. https://doi.org/10.1103/RevModPhys.83.11

[96] Meyer, B. (1954). "On the Symmetries of Spherical Harmonics." *Canadian Journal of Mathematics* **6**, 135–157. https://doi.org/10.4153/CJM-1954-016-2

[97] Strikwerda, J. C. (2004). *Finite Difference Schemes and Partial Differential Equations*. SIAM. https://doi.org/10.1137/1.9780898717938

[98] Trefethen, L. N. (1982). "Group Velocity in Finite Difference Schemes." *SIAM Review* **24**, 113–136. https://doi.org/10.1137/1024038

[99] Weinberg, S. (1995). *The Quantum Theory of Fields, Volume 1: Foundations*. Cambridge University Press. https://doi.org/10.1017/CBO9781139644167

AI Assistance Disclosure

This research project used research-grade commercial models, including Anthropic's Fable and OpenAI's GPT-6 Astra, for research support, software development, editing, and synthesis. The authors are responsible for the paper's claims, methods, and final text.